

Theory of hydrodynamic forces in electric double layers

C. Cramail, R. Lhermerout and E. Charlaix†

Laboratoire Interdisciplinaire de Physique, Université Grenoble-Alpes, UMR 5588, 38402 Saint-Martin-d'Hères, France

(Received xx; revised xx; accepted xx)

We present a theory of the hydrodynamic forces in the drainage flow of an electrolyte between a sphere and a plane with charged surfaces. Our theory considers a thin electrolyte film which is at all times in local equilibrium across its thickness. In addition to the usual lubrication force we explicit the electro-kinetic force due to the transport of the diffuse electrical charges as well as the diffusio-kinetic force due to the transport of the excess ion concentration in the Electrostatic Double Layers (EDL's). Our general formalism covers both the case of non-overlapping EDL's and of overlapping EDL's. We study more specifically the mechanical impedance induced by an oscillatory motion of small amplitude of the surfaces. Among our main results, we show that the increase in damping due to the electro-kinetic effect is not monotonic with the surface charge, and we predict a diffusio-kinetic stiffness with a long range decay in $1/D^4$ susceptible to overcome the stiffness of the equilibrium Derjaguin-Landau-Verwey-Overbeek force. The comparison of our results with experiments could allow one to confront the theories of electrolyte transport in the Electrostatic Double Layers without adjustable parameters.

1. Introduction

The electrostatic and hydrodynamic properties of the solid-liquid interface are at the core of a wide range of biological processes and industrial applications, such as those involving the stability of colloidal suspensions or membrane filtration. This ubiquity justifies the abundance of research conducted on this topic for over a century, at the crossroads of physics, chemistry, and biology. In the context of the necessary decarbonization of our energy sources and growing tensions over freshwater access, a better understanding of equilibrium and transport at the solid-liquid interface has once again become crucial (Bocquet & Charlaix 2010; Siria *et al.* 2017; Bocquet 2020; Gonella *et al.* 2021).

In the early 1850s, Helmholtz was the first to describe the charge separation occurring at the interface between a dielectric solid and an ionic solution. He introduced the term electric double layer (EDL) to refer to the electrical capacitance formed between the charged surface and the counterions in the interfacial layer of the solution. Later, in the early 1910s, Gouy and Chapman independently derived the distributions of electrostatic potential and ionic concentrations at the interface by solving the so-called Poisson-Boltzmann equation, which predicts their exponential decay away from the interface. The DLVO equilibrium force – named after Derjaguin, Landau, Verwey, and Overbeek – was proposed 30 years later based on Gouy-Chapman (GC) theory to describe the stability of colloidal suspensions, with significant industrial implications. Although widely used, the DLVO theory – and, by extension, GC theory – was only experimentally tested in the

† Email address for correspondence: elisabeth.charlaix@univ-grenoble-alpes.fr

late 1970s using the Surface Force Apparatus (SFA), which had been invented a decade earlier by Tabor, Winterton, and Israelachvili (Israelachvili 2011; Tabor & Winterton 1969; Israelachvili & Adams 1978; Horn *et al.* 1989). Measurements showed that GC theory accurately describes reality beyond a few nanometers from the dielectric surface when the solution is sufficiently dilute, typically at concentrations below 1 M.

In the molecular layer adjacent to the surface, which deviates from Gouy-Chapman behavior and is traditionally referred to as the Stern layer, capacitance measurements instead suggest a linear decay of the electrostatic potential. Unlike the so-called diffuse layer, which is well described by GC theory, the Stern layer remains largely enigmatic (Bourg *et al.* 2017; Liu *et al.* 2018b; Wang *et al.* 2024). Today, the term EDL is commonly used to describe this division of the interfacial solution into two layers based on the validity of GC theory, but here, we will use it in Helmholtz’s original sense, excluding the Stern layer from our discussion.

So far, lateral transport at the interface has mainly been described using classical transport equations (with the mean-field approximation for electrostatic interactions) – the Stokes equation for the liquid and the Nernst-Planck equation (with advection) for the ions – within the electric double layer. Smoluchowski, a pioneer in the quantitative description of electrokinetic phenomena, originally derived an expression for the electroosmotic flow rate and streaming current by applying the Stokes equation within the electric double layer, even though he did not know the equilibrium distributions at the time, in 1903 (Smoluchowski 1904). Unlike Smoluchowski, expressions for diffusio-electrokinetic interfacial transport (coupled transport of volume, charge, and solute) have been used for over a century, particularly in colloidal science, assuming equilibrium in the direction normal to the interface, governed by GC theory, with a surface charge identical to that of the overall equilibrium (Gross & Osterle 1968; Prieve *et al.* 1984). For instance, Smoluchowski’s expression for electrophoretic velocity is used to measure a zeta potential, equal to the surface electrostatic potential in the absence of slip, from which a surface charge is deduced using Grahame’s equilibrium relation (1953), which follows from GC theory (Lyklema 1994; Bonthuis & Netz 2012; Siria *et al.* 2013; Hartkamp *et al.* 2018). However, the surface charge thus deduced is never directly compared to a direct measurement of the GC surface charge at global equilibrium. Furthermore, the no-slip boundary condition is potentially used inappropriately, as the hydrodynamic boundary condition is rarely measured (Bocquet & Barrat 2007).

Yet, the surface charge deduced from electrophoresis measurements using the aforementioned classical theory can differ by several orders of magnitude from the intrinsic surface charge measured by titration. Surface charge measurements based on conductivity, which rely on the same classical theoretical framework, sometimes yield values even more divergent from the other two (Lyklema 1994; Bonthuis & Netz 2012; Siria *et al.* 2013; Hartkamp *et al.* 2018). In 2012, Netz and collaborators proposed an interpretation for the multiplicity of experimental surface charges, inspired by molecular dynamics simulations. Using viscosity and dielectric constant profiles defined by simple Heaviside functions (step-like profiles) from the surface, the authors reproduced the relative experimental behaviors of the three aforementioned surface charges. However, this avenue requires further investigation, particularly through additional experimental tests.

Despite the experimental advancements since Smoluchowski, which have brought increasingly greater sensitivity to surface effects, the classical description of diffusio-electrokinetic phenomena still lacks direct experimental validations. We believe that dynamic SFA and colloidal probe AFM (CP-AFM) measurements, combined with equilibrium measurements, could address this gap. The SFA is indeed the instrument of choice for measuring GC surface charge based on DLVO theory. Moreover, its dynamic

version, along with its counterpart, the CP-AFM, has demonstrated its ability to measure viscous forces and hydrodynamic boundary conditions (Cottin-Bizonne *et al.* 2005; Maali *et al.* 2008; Garcia *et al.* 2016; Lizée *et al.* 2024). However, a model describing diffusio-electrokinetic interfacial transports during drainage of a thin film of an ionic solution in SFA or CP-AFM is still lacking.

To be more precise, several authors have investigated the hydrodynamic forces exerted upon drainage of a thin film of ionic solution in sphere-plan geometry. Their various studies predict that these forces have a purely dissipative nature, originating from electro-viscous effects. In 1990, Bike and Prieve calculated, at large sphere-plane separations, the first correction term to the Reynolds force, which results from the pressure-driven flow within the liquid film (Bike & Prieve 1990). More recently, Würger and collaborators analytically derived all subsequent correction terms (Rodríguez Matus *et al.* 2022). However, their model does not provide an analytical expression for the force outside this asymptotic regime. Moreover, these authors entirely neglect concentration gradients and ion transport by diffusion – an assumption that requires further validation. Finally, in 2020, Mugele and collaborators developed a model to explain their observations of electro-viscous forces in dynamic AFM. In their model, ion transport by convection is considered negligible compared to transport by diffusion and migration – an assumption valid in their case, as they worked with an AFM tip of approximately $1\ \mu\text{m}$ in radius (Zhao *et al.* 2020; Liu *et al.* 2018a). However, this model is not suitable for describing the transport mechanisms involved in dynamic SFA and certain CP-AFM with larger probes.

In this paper, we propose a model based on the aforementioned classical framework for the normal hydrodynamic forces measured in SFA or CP-AFM, in the linear response regime, during drainage of a thin film of an ionic solution. The film is considered to be at equilibrium along its thickness. Coupled transports of volume, charge, and solute are all taken into account. Our model is built on a single surface charge: the equilibrium surface charge as described by the Gouy-Chapman electric double layer theory. However, considering a surface charge that varies with the thickness of the film is not an obstacle. The no-slip hydrodynamic boundary condition at the walls is also adopted.

The paper is organized as follows. Sec. 2 presents the equations governing the drainage of a thin film of ionic solution and derives the total force within the Derjaguin approximation. These equations are then simplified in Sec. 3 by assuming local equilibrium across the film thickness. In Sec. 4, we calculate the response force to a surface harmonic oscillation in the linear response regime, and we identify the different physical mechanisms contributing to the mechanical impedance. In Sec. 5, we analyse the contribution of the electro-kinetic effects, while Sec. 6 focuses on the forces generated by diffusio-kinetic mechanisms. Finally, Sec. 7 establishes our conclusions.

2. Electro-hydrodynamic forces in the sphere-plane geometry: the Derjaguin approximation

2.1. General framework of the model

Our model describes applications such as dynamic SFA or colloidal probe AFM. We consider two solid spheres of same radius $2R$, physically identical to each other, located at a small distance $D \ll R$ the one from the other. In the frame of the Derjaguin approximation and related approximations developed below, this geometry is equivalent to a sphere of radius R and a plane. We assume a full symmetry around the axis Oy defined by the sphere centers with the origin O located at mid-distance of the two spheres,

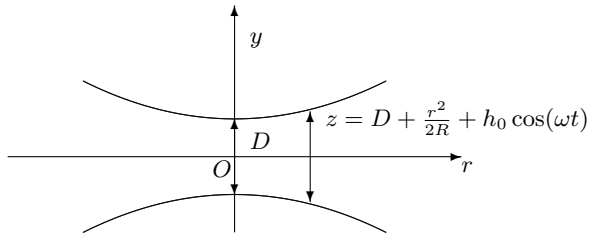


Figure 1: Schematics of the system geometry: an electrolytic solution is confined between two identical spheres of total curvature $1/R$ and whose separation distance is oscillating.

as well as a plane symmetry across $y = 0$, and we use the cylindrical coordinates (O, r, y) . The gap between the surfaces at a distance r of the Oy axis is noted z . The system defined in this manner is depicted in Fig. 1.

The solids are immersed in a solution of monovalent electrolyte of number density n_o (number of cations and anions per unit volume) and their surface are assumed to bare a uniform surface charge σ . The spheres are oscillated harmonically in the normal direction around their nominal position, so that the gap $D(t)$ is:

$$D(t) = D + h_0 \cos(\omega t) \quad h_0 \ll D \ll R$$

The quantity of interest is the hydrodynamic force F normal to the surfaces, and more specifically the linear force response with respect to the oscillation amplitude h_0 :

$$Z(D, \omega) = -\frac{F_\omega}{h_0} \quad F(D, t) = F_{eq}(D) + \Re[F_\omega e^{i\omega t}] + o(h_0^2)$$

where the suffix *eq* refers to the equilibrium situation ($h_0 = 0$). We choose to use a negative sign to define Z in order to get positive real and imaginary part for usual stiffness and dissipative components. We will consider here only the contributions to the force related to hydrodynamics and electrokinetics, at the exclusion of Van der Waals forces and solvation forces, and we will neglect the possible elastic deformation of the solid surfaces. In these conditions the complex amplitude $Z(D, \omega)$ defines the electrohydrodynamic impedance of the system.

Our model uses the standard formulation of the electrokinetic theory in the regime of slowly varying fields, that is neglecting the magnetic fields and wave propagation. The transport of ions is governed by the Poisson-Nernst-Planck equation, and we will note n^+ , n^- the number density of cations and anions, D^+ , D^- their diffusion coefficient, and $\mu^+ = k_B T \ln n^+ / n_o + eV$, $\mu^- = k_B T \ln n^- / n_o - eV$ their electro-chemical potential, where T is the temperature, k_B the Boltzmann constant, and e the elementary charge. We will also use the non-dimensional electrical potential $\psi = eV / k_B T$.

In SFA and AFM applications, the Reynolds number is essentially very low. An upper limit is $Re < h_o \omega R / \eta$ with η the liquid viscosity. With an amplitude h_o limited to 10nm, a frequency of the kHz, a millimetric radius of curvature and the viscosity of water, the Reynolds hardly reaches 10^{-4} . The flow will thus be described by the incompressible

Stokes equation, which we write using the hydrodynamic stress tensor:

$$\mathbf{S}^{\mathcal{H}} = -P\bar{\bar{I}} + \frac{\eta}{2}(\bar{\nabla}\vec{v} + {}^t\bar{\nabla}\vec{v}) \quad |y| < z/2 \quad (2.1)$$

where \vec{v} is the flow velocity, $\bar{\bar{I}}$ the identity matrix, and P the pressure in excess to the atmospheric pressure. We will also use the electrostatic Maxwell stress tensor:

$$\mathbf{S}^{\mathcal{M}} = \varepsilon_i \left(-\frac{\|\bar{\nabla}V\|^2}{2}\bar{\bar{I}} + \bar{\nabla}V \otimes \bar{\nabla}V \right) \quad \begin{cases} \varepsilon_i = \varepsilon_l & \text{if } |y| < z/2 \\ \varepsilon_i = \varepsilon_s & \text{if } |y| > z/2 \end{cases} \quad (2.2)$$

where ε_l , ε_s are the dielectric permittivities respectively of the liquid and of the solids. With these notations the conservation laws and Poisson-Nernst-Planck-Stokes equations write:

$$\nabla^2 V = -\frac{e(n^+ - n^-)}{\varepsilon_l} \quad |y| < \frac{z}{2} \quad \nabla^2 V = 0 \quad |y| > \frac{z}{2} \quad (2.3a)$$

$$\frac{\partial n^\pm}{\partial t} = \text{div} j^\pm \quad \text{div} \vec{v} = 0 \quad (2.3b)$$

$$j^\pm = -\frac{D^\pm}{k_B T} n^\pm \bar{\nabla} \mu^\pm + n^\pm \vec{v} \quad (2.3c)$$

$$\text{div}(\mathbf{S}^{\mathcal{M}} + \mathbf{S}^{\mathcal{H}}) = \vec{0} = -\bar{\nabla}P + \eta \nabla^2 \vec{v} - e(n^+ - n^-)\bar{\nabla}V \quad (2.3d)$$

The boundary conditions at the symmetry plane $y = 0$ also noted with the subscript m, correspond to invariance by the transformation $y \rightarrow -y$:

$$y = 0 : \quad 0 = v_y = \frac{\partial V}{\partial y} = \frac{\partial \mu^\pm}{\partial y} = \frac{\partial v_r}{\partial y} = 0 \quad (2.4)$$

At the liquid solid interface $y = z/2$ also noted with the subscript w, we will assume: i) a no-slip boundary condition, ii) no ion source, iii) the continuity of the electrical potential and the Maxwell-Gauss equation for the normal component of the electrical displacement. These boundary conditions at the solid interface write:

$$\vec{v}_s = -h_0 \omega \sin \omega t \vec{e}_y \quad (2.5a)$$

$$\bar{\nabla} \mu^\pm|_w \cdot \vec{n} = 0 \quad (2.5b)$$

$$V_{w-} = V_{m+} = V_w \quad (2.5c)$$

$$-\varepsilon_s \bar{\nabla} V|_{w+} \cdot \vec{n} + \varepsilon_l \bar{\nabla} V|_{w-} \cdot \vec{n} = \sigma \quad (2.5d)$$

In the following we will ignore charge regulation effects and consider that σ is uniform and non variable. Without loss of generality we will set $\text{sgn}(\sigma)=1$.

Finally the total stress is continuous through the interface. The force $F = \vec{F} \cdot \vec{e}_y$ acting on the upper sphere is obtained formally from the force balance:

$$\vec{F} \cdot \vec{e}_y - \int_0^\infty \vec{e}_y \cdot (\mathbf{S}_{w+}^{\mathcal{M}} \vec{n}) 2\pi r dr = - \int_0^\infty \vec{e}_y \cdot [(\mathbf{S}^{\mathcal{H}} + \mathbf{S}^{\mathcal{M}})|_{w-} \vec{n}] 2\pi r dr \quad (2.6)$$

Our models calculates the linear force response within two further approximations:

- the Derjaguin approximation and its consequences discussed in next paragraph
- the hypothesis of local thermodynamic equilibrium across the thickness z of the liquid film, developed in section 3

2.2. The Derjaguin approximation

The Derjaguin approximation assumes that the force acting on surface elements at a distance z of each other becomes negligible when $z \gtrsim \lambda \ll R$. The characteristic lengths

setting the magnitude of λ , are the Debye's length ℓ_D which sets the range of electrostatic interactions, and the smallest distance D between the surfaces, which sets the range of the hydrodynamic interactions. In these conditions the interacting surfaces are always almost parallel to each other, so that $\vec{n} \approx \vec{e}_y$, and \vec{n} has to be replaced by \vec{e}_y in the boundary conditions (2.5b, 2.5d, 2.6). Also according to the Derjaguin approximation, the gap between the surfaces reduces to the parabolic approximation:

$$z(r, t) = z(r) + h_0 \cos(\omega t) \quad z(r) = D + \frac{r^2}{2R} \quad (2.7)$$

Hence the Derjaguin approximation describes as well a sphere of radius R and a plane.

Because of the hypothesis $\lambda \ll R$, the variation of the physical quantities in the liquid film along the r axis occurs on a radial distance of order $\sqrt{R\lambda}$ much larger than the distance of variation along the Oy axis, which is of order of some λ . Thus for any quantity a which varies significantly across the thickness the liquid film we have:

$$\left| \frac{\partial a}{\partial r} \right| \ll \left| \frac{\partial a}{\partial y} \right| \quad |y| \leq \frac{z}{2} \quad (2.8)$$

A first important consequence of the Derjaguin approximation is that the Poisson's equation in the liquid (2.3a, $|y| < z/2$) and its boundary condition (2.5d) become:

$$\frac{\partial^2 V}{\partial y^2} = -\frac{e(n^+ - n^-)}{\varepsilon_\ell} \quad \frac{\partial V}{\partial y} \left[\left(\frac{z}{2} \right)^- \right] = \frac{\sigma}{\varepsilon_\ell} \quad (2.9)$$

It is indeed shown in the Appendix that the normal field in the dielectric is of the same order of magnitude as the radial field $(\partial V / \partial r)[(z/2)^-]$ which is neglected. By integrating eq. (2.9) along the y -direction one sees that the Derjaguin approximation implies the local electroneutrality of the electrolyte film together with the surfaces:

$$\int_0^{z(t)/2} e(n^+ - n^-)(r, y, t) dy = -\sigma \quad (2.10)$$

As the surfaces are almost parallel to each other in the interaction region, $\vec{n} \approx \vec{e}_y$. Together with the inequality (2.8), the normal component of the Maxwell stress tensor at the interface reduces to:

$$\mathbf{S}_w^M \vec{n} \approx S_{yy}^M \vec{e}_y \approx \frac{\varepsilon_i}{2} \left(\frac{\partial V}{\partial y} \right)^2 \vec{e}_y$$

It is thus negligible in the dielectric. The expression of the force (2.6) becomes:

$$\begin{aligned} F &= - \int_0^\infty 2\pi r (S_{yy}^M + S_{yy}^H)(r, \frac{z^-}{2}) dr \\ &= - \int_0^\infty 2\pi r \left(-P + 2\eta \frac{\partial v_y}{\partial y} + \frac{\varepsilon_\ell}{2} \left(\frac{\partial V}{\partial y} \right)^2 \right) (r, \frac{z^-}{2}) dr \end{aligned} \quad (2.11)$$

We show in appendix that within the Derjaguin approximation the force reduces to:

$$F = \int_0^\infty 2\pi r P(r, 0) dr \quad (2.12)$$

2.3. Equilibrium state

In the following we will linearize the dynamic force to the first order in h_0 around the equilibrium state. The latter has been described by and leads to the well-known DLVO

force. At equilibrium the electro-chemical potential of the ions are uniform: $\mu_{eq}^{\pm} = 0$. The ion densities obey the Boltzmann law $n_{eq}^{\pm} = n_o e^{\mp\psi_{eq}}$ where the reduced potential $\psi_{eq} = eV_{eq}/k_B T$ is governed by the Poisson-Boltzmann equation:

$$\frac{\partial^2 \psi_{eq}}{\partial y^2} = \frac{\sinh \psi_{eq}}{\ell_D^2} \quad \ell_D^2 = \frac{\varepsilon_l k_B T}{2e^2 n_o} = \frac{1}{8\pi \ell_B n_o} \quad (2.13)$$

and ℓ_D is the Debye's length. The analytical solution for ψ_{eq} is (Behrens & Grier 2001):

$$\psi_{eq}(r, y) = \psi_{eq,m}(r) - \ln \left[\text{cd} \left(y/2\ell_D \sqrt{k} \right) \right]^2 \quad k = e^{-\psi_{eq,m}} \quad (2.14)$$

for a positive surface charge. The subscript m refers to the middle position $y = 0$ and $\text{cd}(u|k^2)$ is the Jacobi elliptical function of argument u and parameter k^2 . The parameter $k^2(z)$ is determined from the boundary condition (2.9) by:

$$2 \cosh \psi_{eq,s} = k \text{cd}^2(z'/2) + \frac{1}{k \text{cd}^2(z'/2)} = k + \frac{1}{k} + \alpha^2 \quad (2.15)$$

$$z' = \frac{z}{2\ell_D \sqrt{k}} \quad \alpha = \frac{2\ell_D}{l_G}$$

We note that k depends only on $(z/\ell_D, \ell_G/\ell_D)$, and the function $\psi_{eq}(y)$ depends on $(y/\ell_D, z(r)/\ell_D, \ell_G/\ell_D)$. Finally the equilibrium pressure is obtained by projecting on the r axis the hydrostatic equation (2.3d) with $\vec{v} = \vec{0}$:

$$\frac{\partial P_{eq}}{\partial r} = 2k_B T n_o \sinh \psi_{eq} \frac{\partial \psi_{eq}}{\partial r}$$

With the value $P_{eq} = \psi_{eq} = 0$ in the reservoir, one finds that $P_{eq} = 2n_o k_B T (\cosh \psi_{eq} - 1)$, and equation (2.12) retrieves the equilibrium DLVO force:

$$F_{eq} = 2n_o k_B T \int_0^{\infty} 2\pi r (\cosh \psi_{eq,m} - 1) dr$$

where $\psi_{eq,m} = \psi_{eq}(y = 0)$ is the reduced potential in the symmetry plane. Using the parabolic approximation $z = D + r^2/2R$ the equilibrium force is written in the usual form

$$F_{eq} = 4\pi R n_o k_B T \int_D^{\infty} (\cosh \psi_{eq,m} - 1) dz \quad (2.16)$$

3. Hypothesis of local equilibrium across the film thickness

3.1. Conditions

Due to the separation of scales, we assume that equilibrium is instantaneously reached along the confinement axis. This assumption is based on the comparison of the working period $2\pi/\omega$ with the relevant ionic diffusion time τ_y normal to the surfaces. A lower limit of τ_y is estimated for a Debye's length $\ell_D \sim 100$ nm, as:

$$\tau_y \sim \frac{\lambda_D^2}{D_{\text{diff}}} \sim \frac{(10^{-7})^2}{10^{-9}} = 10^{-5} \text{ s} \quad (3.1)$$

This assumption therefore holds true in dynamic SFA with a typical working frequency of 5 Hz to 500 Hz. However in colloidal probe AFM, the working frequency should not exceed 1 kHz.

3.2. Thermodynamic potentials

Under this local equilibrium assumption, the electrochemical potential μ^+ and μ^- of the ions are uniform across the thickness of the electrolyte film. We introduce the sum and difference potentials as well as the equivalent concentration $n(r, t)$ as:

$$\mu_s = \frac{\mu^+ + \mu^-}{2} = k_B T \ln \frac{n(r, t)}{c_o} \quad W = \frac{\mu^+ - \mu^-}{2e} \quad (3.2a)$$

$$\chi(r, y, t) = \frac{e}{k_B T} (V - W) \quad (3.2b)$$

The equivalent ion density $n(r, t)$ is the ion density of a virtual reservoir at 0-potential that would be in equilibrium with the film at radial distance r and time t . The sum and difference concentration of ions are defined as:

$$n_s = n^+ + n^- = 2n(r, t) \cosh \chi \quad n_e = n^+ - n^- = -2n(r, t) \sinh \chi \quad (3.3)$$

The potentials μ_s and W are uniform over the thickness. Therefore the reduced potential χ satisfies the Poisson equation (2.9) with the expression (3.3) for the charge density:

$$\frac{\partial^2 \psi}{\partial y^2} = \frac{\partial^2 \chi}{\partial y^2} = \frac{n(r, t) \sinh \chi}{\ell_D^2} \quad \frac{\partial \chi}{\partial y} \Big|_{z(r, t)/2} = \frac{\partial \psi}{\partial y} \Big|_{z(r, t)/2} = -\frac{2}{\ell_G} \quad (3.4)$$

This set of equation and boundary condition is equivalent to the one defining the equilibrium electrical potential ψ_{eq} , but with a local Debye's length $\lambda_D(r, t)$ and a boundary condition applied at the moving wall $z(t)$. The solution is thus:

$$\chi(r, y, t) = \psi_{eq}(y, z(r, t), \lambda_D) \quad \lambda_D(r, t) = \frac{\ell_D}{\sqrt{n(r, t)}} = \ell_D e^{-\mu_s(r, t)/2k_B T} \quad (3.5)$$

This means that the dynamic concentration profiles (3.3) reach instantaneously the equilibrium value that would prevail if the reservoir concentration was $n(r, t) = n_o e^{\mu_s/k_B T}$ and the distance between the surface $z(t)$.

The transport equations are written in terms of the sum and difference variables by introducing the average diffusion coefficient:

$$D_s = \frac{D^+ + D^-}{2} \quad \delta = \frac{D^+ - D^-}{D^+ + D^-} \quad D^\pm = D_s(1 \pm \delta) \quad (3.6)$$

Using equations (3.2) and (3.3) we get the identity:

$$e(n^+ - n^-) \vec{\nabla} V = e n_e \vec{\nabla} W + n_s \vec{\nabla} \mu_s - k_B T \vec{\nabla} n_s \quad (3.7)$$

and write eq (2.3b, 2.3c) and (2.3d) as:

$$\frac{\partial n_s}{\partial t} = -\text{div} \vec{j}_s \quad \frac{\partial n_e}{\partial t} = -\text{div} \vec{j}_e \quad \text{div} \vec{v} = 0 \quad (3.8a)$$

$$\vec{j}_s = n_s \vec{v} - \frac{D_s}{k_B T} \left\{ (n_s + \delta n_e) \frac{d\mu_s}{dr} + e(n_e + \delta n_s) \frac{dW}{dr} \right\} \quad (3.8b)$$

$$\vec{j}_e = n_e \vec{v} - \frac{D_s}{k_B T} \left\{ (n_e + \delta n_s) \frac{d\mu_s}{dr} + e(n_s + \delta n_e) \frac{dW}{dr} \right\} \quad (3.8c)$$

$$\eta \frac{\partial^2 v_r}{\partial y^2} = \frac{d\Pi}{dr} + e n_e \frac{dW}{dr} + (n_s - 2n) \frac{d\mu_s}{dr} \quad (3.8d)$$

$$\Pi = P - (n_s - 2n) k_B T \quad (3.8e)$$

In the Stokes equation (2.3d) the radial components $\Delta_r \vec{v}$ has been neglected according

to the Derjaguin approximation, to obtain (3.8d). We show in the Appendix that the osmotically compensated pressure Π defined in (3.8e) is uniform across the film thickness.

The three terms of the r.h.s. of the Stokes equation (3.8d) outline the three contributions to the flow. The first term $d\Pi/dr$, uniform in the section, induces a Poiseuille-like velocity profile: this is the pressure driven flow. The second term is the effective electrical driving force, as $-dW/dr$ is the radial electrical field which develops across the liquid film. This term vanishes outside of the EDLs as the volume charge en_e , it is the source of an electro-osmotic flow. The third term also eventually vanishes outside of the EDLs, it induces a diffusio-osmotic flow driven by the concentration gradient $d\mu_s/dr = (k_B T/n)dn/dr$ (Prieve *et al.* (1984)).

3.3. Conservation laws integrated over the thickness

The above equations are integrated across the thickness by defining:

$$N_s(r, t) = \int_0^{z(t)/2} (n_s - 2n_o) dy \quad N_e(r, t) = \int_0^{z(t)/2} n_e dy = -\frac{\sigma}{e} \quad (3.9)$$

$$J_{s,e} = \int_0^{z(t)/2} \vec{j}_{s,e} \cdot \vec{e}_r dy \quad J_v = \int_0^{z(t)/2} v_r(y) dy \quad (3.10)$$

The constant value of N_e reflects the global electro-neutrality (2.10).

In view of equations (3.8) it is clear that the fluxes (J_v , J_s , J_e) are linear functions of the gradients of the thermodynamic potential (Π , μ_s , W). We show in the appendix that these fluxes are related to the above gradients by the 3x3 symmetric matrix \mathbf{T} as:

$$\begin{pmatrix} J_v \\ J_s - 2n(r, t)J_v \\ eJ_e \end{pmatrix} = -\mathbf{T} \frac{\partial}{\partial r} \begin{pmatrix} \Pi \\ \mu_s \\ W \end{pmatrix} \quad \mathbf{T} = \frac{\mathbf{K}}{\eta} + \frac{D_s \mathbf{L}}{k_B T} \quad (3.11a)$$

$$K_{ij} = \int_0^{z(t)/2} \Gamma_i \Gamma_j dy \quad (i, j) \in (v, s, e) \quad (3.11b)$$

$$\Gamma_s(y) = \int_0^y (n_s - 2n) dy \quad \Gamma_e(y) = \int_0^y en_e dy \quad \Gamma_v(y) = y \quad (3.11c)$$

$$L_{ve} = L_{ev} = L_{vs} = L_{sv} = 0 \quad (3.11d)$$

$$L_{ss} = \frac{L_{ee}}{e^2} = N_s + \frac{z}{2} + N_e \delta \quad L_{se} = L_{es} = e \left[N_e + (N_s + \frac{z}{2}) \delta \right] \quad (3.11e)$$

The two components \mathbf{K} and \mathbf{L} of the transport matrix \mathbf{T} reflect the convective and the diffusive contributions in the flux expressions (3.8b) and (3.8c).

The three conservation laws (3.8a) integrated over the thickness write as:

$$\frac{\partial(z/2)}{\partial t} = \frac{\dot{D}}{2} = -\frac{1}{r} \frac{\partial r J_v}{\partial r} \quad (3.12a)$$

$$\frac{\partial N_e}{\partial t} = \int_0^{z(t)/2} \left(\frac{\partial c_e}{\partial t} + \frac{\partial j_{e,y}}{\partial y} \right) dy = -\frac{1}{r} \frac{\partial r J_e}{\partial r} \quad (3.12b)$$

$$\frac{\partial N_s}{\partial t} = \int_0^{z(t)/2} \left(\frac{\partial c_s}{\partial t} + \frac{\partial j_{s,y}}{\partial y} \right) dy - \frac{\partial z}{2 \partial t} = -\frac{1}{r} \frac{\partial r (J_s - 2n J_v)}{\partial r} - \frac{2}{r} \frac{\partial r (n - n_o) J_v}{\partial r} \quad (3.12c)$$

These equations are further reduced by noting that $\partial z / \partial t = -h_0 \omega \sin \omega t$ does not depend on r , therefore the first equation can be integrated once, leading to $J_v = -(r/4)(\partial z / \partial t)$. Furthermore in the absence of charge-regulation phenomena N_e is constant (see eq. 2.10), and the second equation integrates in $J_e = 0$ as J_e does not diverge at $r = 0$. Using the relations (3.11a) and eliminating dW/dr , equations (3.12a) and (3.12c)

become a set of two second-order non-linear differential equations:

$$\left(T_{vv} - \frac{T_{ev}^2}{T_{ee}}\right) \frac{\partial \Pi}{\partial r} + \left(T_{vs} - \frac{T_{ev}T_{es}}{T_{ee}}\right) \frac{\partial \mu_s}{\partial r} = \frac{r}{4} \frac{\partial z}{\partial t} \quad (3.13a)$$

$$\frac{1}{r} \frac{\partial}{\partial r} \left[r \left(T_{vs} - \frac{T_{ev}T_{es}}{T_{ee}}\right) \frac{\partial \Pi}{\partial r} + r \left(T_{ss} - \frac{T_{es}^2}{T_{ee}}\right) \frac{\partial \mu_s}{\partial r} + \frac{r^2 n_o (e^{\mu_s/k_B T} - 1)}{2} \frac{\partial z}{\partial t} \right] = \frac{\partial N_s}{\partial t} \quad (3.13b)$$

Note that the coefficient T_{ee} indeed represents the conductance of the electrolyte film and cannot vanish.

The quantity N_s and the elements of \mathbf{T} are given by the equations (3.3,3.5,3.9) and (3.11) as a function of $z(t)$ and $M_s(t)$. Therefore the equations (3.13) provide a fully determined set of two non-linear differential equations to be solved with the boundary conditions $\Pi = \mu_s = 0$ at $r = \infty$ and finite second derivative in $r = 0$. The pressure is then determined from (3.8e), giving the electro-hydrodynamic force:

$$F(t) = \int_0^\infty 2\pi r (\Pi + 2n(r,t)k_B T [\cosh \chi(r,0,t) - 1]) dr \quad (3.14)$$

The term $2k_B T n(r,t) [\cosh \chi(r,0,t) - 1]$ is the osmotic pressure at the level of the mid-plane. This term decays exponentially with the sphere-plane distance with a screening length equal to the dynamic Debye's length, and represents the direct interaction of the EDL's in dynamic conditions. The term in Π corresponds to the long-range hydrodynamic contribution to the force, including all the effects of charge and ions transport described in equations (3.13).

4. Linear response and contributions to the mechanical impedance

4.1. Linearized transport equations

At small h_0 the above equations are linearized in h_0 keeping in mind that terms of order 0 do not vary in time and terms of order 1 are harmonic oscillations of frequency ω . In the following, quantities which vanish at equilibrium such as the fluxes $[J]$ and the thermodynamic potentials, are noted through their complex amplitude as $f(y,r,t) = \text{Re}[f(r,y)e^{i\omega t}]$, with $\partial/\partial t = i\omega$. Quantities which do not vanish at equilibrium will be noted $f(r,y,t) = f_{eq}(r,y) + \text{Re}[df(r,y)e^{i\omega t}]$ with $df \in \mathbb{C}$. An exception will be the equilibrium film thickness noted $z_{eq}(r) = z(r) = D + r^2/R$ (2.7).

Equations (3.13) are re-written taking into account that:

(i) the thermodynamic potentials Π and μ_s are of order 1 in h_0 . We introduce non-dimensional potentials scaled by the amplitude h_0 as:

$$m_v = \frac{\Pi}{2n_o k_B T} \frac{\ell_D}{h_0} \quad m_s = \frac{\mu_s}{k_B T} \frac{\ell_D}{h_0} \quad m_e = \frac{eW}{k_B T} \frac{\ell_D}{h_0} \quad (4.1)$$

and non-dimensional lengths scaled by $2\ell_D$, such as $\tilde{z} = z/2\ell_D$, $\tilde{y} = y/2\ell_D$ and $\tilde{D} = D/2\ell_D$, etc...

(ii) the term $(e^{\mu_s/k_B T} - 1)\partial z/\partial t$ in the l.h.s of (3.13b), of order h_0^2 , is not kept

(iii) in the linearized equations the transport matrix \mathbf{T} restricts to its *equilibrium value* $\mathbf{T} = \mathbf{T}_{eq}$. This means that the T_{ij} have to be calculated with the equilibrium concentration $c_{s,eq} = \cosh \psi_{eq}$ and $c_{e,eq} = -\sinh \psi_{eq}$. A dimensionless transport matrix $\mathbf{t} = (t_{ij})$ is

introduced as:

$$t_{ij} = 2 \int_0^{\tilde{z}/2} \tilde{\Gamma}_i(\tilde{y}) \tilde{\Gamma}_j(\tilde{y}) d\tilde{y} + 2\kappa \tilde{L}_{ij} \quad i, j \in (v, s, e) \quad (4.2a)$$

$$\kappa = \frac{D_s \pi \eta \ell_B}{k_B T} \quad \forall i \quad \tilde{L}_{vi} = 0 \quad (4.2b)$$

$$\tilde{\Gamma}_v(\tilde{y}) = \tilde{y} \quad \tilde{\Gamma}_s(\tilde{y}) = \int_0^{\tilde{y}} (\cosh \psi_{eq} - 1) d\tilde{y}' \quad \tilde{\Gamma}_e(\tilde{y}) = \int_0^{\tilde{y}} (-\sinh \psi_{eq}) d\tilde{y}' \quad (4.2c)$$

$$\tilde{L}_{se} = \tilde{L}_{es} = \tilde{\Gamma}_e\left(\frac{\tilde{z}}{2}\right) + \delta\left(\tilde{\Gamma}_s\left(\frac{\tilde{z}}{2}\right) + \frac{\tilde{z}}{2}\right) \quad \tilde{L}_{ss} = \tilde{L}_{ee} = \tilde{\Gamma}_s\left(\frac{\tilde{z}}{2}\right) + \frac{\tilde{z}}{2} + \delta\tilde{\Gamma}_e\left(\frac{\tilde{z}}{2}\right) \quad (4.2d)$$

where $\ell_B = e^2/4\pi\epsilon_l k_B T$ is the Bjerrum length. In these units the reduced Poiseuille coefficient is $t_{vv} = \tilde{z}^3/12$. The non-dimensional diffusivity κ is the ratio of the average molecular diffusion coefficient D_s to the osmotic diffusion coefficient $K_{DO} = k_B T/\pi\eta\ell_B$ which scales the bulk diffusio-osmotic velocity in presence of a concentration gradient as $v_{DO} \propto K_{DO} \vec{\nabla} \ln C$ (Anderson (1989); Siria *et al.* (2013)).

(iv) as \mathbf{T}_{eq} (resp. \mathbf{t}) depends actually on $z = D + r^2/2R$ (resp. \tilde{z}), the differential elements in (3.13) are replaced as $r\partial r = Rdz$ and $r/\partial r = 2(z - D)/dz$ (resp. $2(\tilde{z} - \tilde{D})/d\tilde{z}$)

(v) at all places and time the dynamic concentration profile $n_s(r, y, t)$ is equal to the equilibrium profile that would be obtained for the time-dependant values of the film thickness $z(r, t) = z(r) + h_o \cos \omega t$ and of the Debye length $\lambda_D(r, t) = \ell_D e^{-\mu_s/2k_B T}$. Therefore the linear response of $\partial N_s/\partial t$ is a linear expression of h_o and μ_s , noted $dN_s(h_o, \mu_s)$. The associated non-dimensional quantity writes $dN_s/h_o n_o = a(\tilde{z}) + b(\tilde{z})m_s$ where the non-dimensional functions $a(\tilde{z})$ and $b(\tilde{z})$ are expressed in appendix.

Under these circumstances equations (3.13) become two 2nd order linear differential equations in Π and μ_s with non-constant coefficients:

$$\left(T_{vv} - \frac{T_{ev}^2}{T_{ee}}\right) \frac{d\Pi}{dz} + \left(T_{vs} - \frac{T_{ev}T_{es}}{T_{ee}}\right) \frac{d\mu_s}{dz} = \frac{i\omega R h_o}{4} \quad (4.3a)$$

$$\frac{d}{dz} \left\{ (z - D) \left[\left(T_{vs} - \frac{T_{ev}T_{es}}{T_{ee}}\right) \frac{d\Pi}{dz} + \left(T_{ss} - \frac{T_{es}^2}{T_{ee}}\right) \frac{d\mu_s}{dz} \right] \right\} = \frac{i\omega R}{2} dN_s \quad (4.3b)$$

to be solved for $z \in [D, \infty[$ with boundary conditions of finite second derivative at $z = D$ and zero value at infinity. The non-dimensional counterpart writes:

$$\left(t_{vv} - \frac{t_{ev}^2}{t_{ee}}\right) \frac{dm_v}{d\tilde{z}} + \left(t_{vs} - \frac{t_{ev}t_{es}}{t_{ee}}\right) \frac{dm_s}{d\tilde{z}} = \frac{i\omega}{\omega_c} \quad (4.4a)$$

$$\frac{d}{d\tilde{z}} \left\{ (\tilde{z} - \tilde{D}) \left[\left(t_{vs} - \frac{t_{ev}t_{es}}{t_{ee}}\right) \frac{dm_v}{d\tilde{z}} + \left(t_{ss} - \frac{t_{es}^2}{t_{ee}}\right) \frac{dm_s}{d\tilde{z}} \right] \right\} = \frac{i\omega}{\omega_c} (a(\tilde{z}) + b(\tilde{z})m_s) \quad (4.4b)$$

$$\omega_c = \frac{2k_B T}{\pi\eta\ell_B R \ell_D} \quad (4.4c)$$

4.2. Contributions to the mechanical impedance

The linear force response obtained from eq. (3.14) writes as:

$$Z = -\frac{F}{h_o} = -2\pi R \int_D^\infty \frac{\Pi}{h_o} dz + 4\pi R n_o k_B T (\cosh \psi_{eq,m}(D) - 1) - 4\pi R n_o \int_D^\infty \frac{\mu_s}{h_o} \left(\cosh \psi_{eq,m} - 1 + \frac{\partial \cosh \psi_{eq,m}}{\partial (\ln n_o)} \right) dz \quad (4.5)$$

These terms are splitted in different contributions according to their physical origin.

-*DLVO stiffness*: according to (4.3), at zero frequency the fields Π and μ_s vanish, and the mechanical impedance resumes to the derivative of the equilibrium DLVO force (2.16):

$$Z(\omega = 0) = Z_{\text{DLVO}} = -\frac{dF_{\text{DLVO}}}{dD} = 4\pi Rk_B T n_o (\cosh \psi_{eq,m}(D) - 1) \quad (4.6)$$

This contribution has no imaginary part and is a pure stiffness.

-*Reynolds damping*: at finite frequency the pressure can be splitted in three terms $\Pi_{\text{Rey}} + \Pi_{\text{EK}} + \Pi_{\text{DK}}$ as:

$$\begin{aligned} \frac{d\Pi_{\text{Rey}}}{dz} &= \frac{i\omega R h_0}{4T_{\text{vv}}} = \frac{6i\omega R h_0 \eta}{z^3} & \frac{d\Pi_{\text{EK}}}{dz} &= \frac{i\omega R h_0}{4} \frac{T_{\text{ve}}^2}{T_{\text{vv}}(T_{\text{vv}}T_{\text{ee}} - T_{\text{ve}}^2)} \\ & & \frac{d\Pi_{\text{DK}}}{dz} &= -\frac{T_{\text{vs}}T_{\text{ee}} - T_{\text{ve}}T_{\text{se}}}{T_{\text{vv}}T_{\text{ee}} - T_{\text{ve}}^2} \frac{d\mu_s}{dz} \end{aligned} \quad (4.7)$$

The term Π_{Rey} gives the so-called Reynolds viscous force exerted by a dielectric liquid drained from the gap between a sphere and a plane:

$$Z_{\text{Rey}} = \frac{6i\pi\eta\omega R^2}{D} \quad (4.8)$$

-*Electro-kinetic damping*: the pressure term Π_{EK} corresponds to the excess viscous dissipation induced by electrokinetic effects in the electrolyte film when all perturbations in the ions concentration are ignored. Indeed, if one neglects the concentration perturbations in the film, equations (3.11) write:

$$\begin{aligned} eJ_e = 0 &= -T_{\text{ve}} \frac{d(\Pi_{\text{Rey}} + \Pi_{\text{EK}})}{dr} - T_{\text{ee}} \frac{dW}{dr} \\ J_v = -\frac{r}{4} \frac{dz}{dt} &= -T_{\text{vv}} \frac{d\Pi_{\text{Rey}}}{dr} = -T_{\text{vv}} \frac{d(\Pi_{\text{Rey}} + \Pi_{\text{EK}})}{dr} - T_{\text{ve}} \frac{dW}{dr} \end{aligned}$$

In other words, the electro-neutrality enforces the streaming current $-T_{\text{ve}}d\Pi/dr$ to be compensated by a conductivity current $-T_{\text{ee}}dW/dr$, which requires a radial electrical field $-dW/dr$ to develop in the liquid film. This electrical field in return induces an electro-osmotic flow rate $-T_{\text{ve}}dW/dr$ which has to be compensated by an additional pressure-driven flow $-T_{\text{vv}}d\Pi_{\text{EK}}/dr$ in order to maintain the prescribed fluid flow. The electrokinetic effect induces a so-called electro-viscous force, calculated for large distance $D \gg 2\ell_D$ by Bike & Prieve (1990) and also Rodríguez Matus *et al.* (2022). Note that this electro-viscous force does not take into account the effect of concentration changes induced by the squeeze flow. It corresponds to a contribution Z_{EK} to the mechanical impedance:

$$\begin{aligned} Z_{\text{EK}} &= \frac{i\omega R}{4} \int_D^\infty \int_z^\infty \frac{T_{\text{ve}}^2 dz}{T_{\text{vv}}(T_{\text{vv}}T_{\text{ee}} - T_{\text{ve}}^2)} = \frac{i\omega}{\omega_c} 8\pi R n_o k_B T Z_{\text{EK}} \\ Z_{\text{EK}} &= \int_{\bar{D}}^\infty d\bar{z} \int_{\bar{z}}^\infty \frac{t_{\text{ve}}^2}{t_{\text{vv}}(t_{\text{vv}}t_{\text{ee}} - t_{\text{ve}}^2)} d\bar{z} \quad \omega_c = \frac{2k_B T}{\pi\eta\ell_B R\ell_D} \end{aligned} \quad (4.9)$$

The electrokinetic impedance Z_{EK} is purely dissipative (imaginary) and strictly proportional to the frequency. For thermodynamic reasons, $T_{\text{vv}}T_{\text{ve}} \geq T_{\text{ve}}^2$ ($t_{\text{vv}}t_{\text{ve}} \geq t_{\text{ve}}^2$), therefore the electrokinetic impedance always corresponds to an excess dissipative force with respect to the nominal Reynolds force. When the fluid conductivity is very large,

$T_{ee} = \infty$, the electric field developed in the film becomes negligible, and Z_{EK} vanishes. Section 5 discusses the properties of the real positive non-dimensional factor \mathcal{Z}_{EK} .

-*Diffusio-kinetic impedance*: all remaining contributions involve perturbations of the equilibrium ion concentration and are gathered in an additional impedance that we name here, somewhat abusively, a diffusion-kinetic contribution Z_{DK} . We show in appendix that the expression $\cosh \psi_{eq,m} - 1 + \partial \cosh \psi_{eq,m} / \partial (\ln n_o)$ appearing in equation (4.5) resumes to the function $a(\tilde{z})$, so that Z_{DK} writes as:

$$\mathcal{Z}_{DK} = - \int_{\tilde{D}}^{\infty} d\tilde{z} \left(a(\tilde{z}) m_s(\tilde{z}) + \int_{\tilde{z}}^{\infty} g(\tilde{z}') \frac{dm_s(\tilde{z}')}{d\tilde{z}'} d\tilde{z}' \right) \quad Z_{DK} = 8\pi R n_o k_B T \mathcal{Z}_{DK} \quad g(\tilde{z}) = \frac{t_{vs} t_{ee} - t_{ve} t_{es}}{t_{vv} t_{ee} - t_{ve}^2} \quad (4.10)$$

where the reduced potential m_s is solution of the 2nd order linear differential equation obtained by decoupling the two equations (4.4):

$$\frac{d}{d\tilde{z}} \left\{ (\tilde{z} - \tilde{D}) \left(h(\tilde{z}) \frac{dm_s}{d\tilde{z}} + \frac{i\omega}{\omega_c} g(\tilde{z}) \right) \right\} = \frac{i\omega}{\omega_c} (a(\tilde{z}) + b(\tilde{z}) m_s) \quad (4.11a)$$

$$h(\tilde{z}) = t_{ss} - \frac{t_{se}^2}{t_{ee}} - \frac{(t_{vs} - t_{ve} t_{se}/t_{ee})^2}{t_{vv} - t_{ve}^2/t_{ee}} \quad \omega_c = \frac{2k_B T}{\pi \eta \ell_B R \ell_D} \quad (4.11b)$$

The first term of \mathcal{Z}_{DK} appearing in equation (4.10) accounts for the modification of the disjunction pressure in the middle-plane due to the perturbed ion concentration. This term is short-ranged as the function $a(\tilde{z})$ vanishes exponentially with $\tilde{z} = z/2\ell_D$. It represents the out-of-equilibrium direct interaction of the EDL's. The second term gathers all the transport effects induced by the concentration gradient $\partial \mu_s / \partial r$. The concentration gradient induces a diffusio-osmotic flow, which in the same way as the electro-osmotic flow, has to be compensated by an additional Poiseuille flow in order to maintain the prescribed flow rate in the liquid film. Furthermore diffusio-osmotic effects contribute to a diffusio-osmotic charge current, which in turn modify the electro-kinetic charge restauration effect in the electrolyte film. These contributions are embeded in the terms $t_{vs} t_{ee} / (t_{vv} t_{ee} - t_{ve}^2)$ and $t_{ve} t_{se} / (t_{vv} t_{ee} - t_{ve}^2)$ of the g function.

As ions can accumulate, Z_{DK} is frequency-dependant with an imaginary as well as a real component. It thus contributes both to the stiffness and to the damping of the global impedance. The frequency behaviour of Z_{DK} is scaled by the system frequency ω_c , associated to the osmotic diffusion time (with diffusion coefficient $K_{DO} = k_B T / \pi \eta \ell_B$) over the lateral extension $\sqrt{R \ell_D}$ of the EDL's contact.

4.3. Summary

In summary our theory describes the mechanical impedance in a drainage flow of a monovalent electrolyte as a function of the normalized distance $\tilde{D} = D/2\ell_D$ and 4 non-dimensional parameters:

- the parameter α characterizes the electrostatic properties of the surfaces in the solution of concentration n_o . More specifically α is related to the nominal surface potential $V_{s,nominal}$ of the surfaces alone (non-interacting) by $\alpha = 2 \sinh(eV_{s,nominal}/2k_B T)$. In water at 300 K, the value $\alpha = 1$ corresponds to a nominal surface potential of 24 mV, $\alpha = 10$ to 115 mV, $\alpha = 100$ to 230 mV.
- the parameter κ characterizes the average diffusion coefficient of the electrolyte. If anions and cations have a similar diffusion coefficient, κ is related to the hydrodynamic radius of the ions defined by the Stokes-Einstein relation $D_s = k_B T / 6\pi \eta r_H$ by $\kappa = \ell_B / 6r_H$ where ℓ_B is the Bjerrum length. For the KCl electrolyte of diffusion coefficient $1.45 \cdot 10^{-9} \text{m}^2/\text{s}$ in water at 300K, $\kappa = 0.7$.

- the parameter δ describes the diffusion contrast between co-ions and the counter-ions. The diffusion coefficient of counter-ions is $D_s(1 - \delta)$.
- the frequency ratio $\beta = \omega/\omega_c$. It is of interest to note that the combination $\beta/\kappa = \omega/\kappa\omega_c = \omega R\ell_D/2D_s$ characterizes the ratio of the diffusion time over the lateral extension of the overlapping EDL's at contact $D = 0$, to the period of the oscillation. The dimensional real and imaginary part of the mechanical impedance write:

$$\Re Z = 8\pi R n_o k_B T \left(\frac{1}{2} [\cosh \psi_{m,eq}(\tilde{D}, \alpha) - 1] + \Re \mathcal{Z}_{DK}(\tilde{D}, \alpha, \beta, \kappa, \delta) \right) \quad (4.12a)$$

$$\Im Z = \frac{6\pi\omega\eta R^2}{D} (1 + \tilde{f}_{EK} + \tilde{f}_{DK}) \quad (4.12b)$$

$$\tilde{f}_{EK}(\tilde{D}, \alpha, \kappa, \delta) = \frac{\tilde{D}}{6} \mathcal{Z}_{EK} \quad \tilde{f}_{DK}(\tilde{D}, \alpha, \beta, \kappa, \delta) = \frac{\tilde{D}}{6\beta} \Im \mathcal{Z}_{DK} \quad (4.12c)$$

5. Properties of the electro-kinetic damping

In the following the non-dimensional electro-kinetic factor \mathcal{Z}_{EK} is calculated by integrating numerically equation 4.9, the transport coefficients being themselves calculated by numerical integration of equations 4.5 with the expressions of $\tilde{T}_{e,s}$ given in Appendix. Details of implementation are given in the Supplementary Informations. We find that at $\tilde{D} \geq 10$ the transport coefficients meet fully the large distance expressions given in Appendix D, and we use these expressions.

5.1. Large distance behaviour.

Electrostatic Double Layers are considered non-overlapping if the distance between the surfaces is very large compared to the Debye's length, $D \gg 2\ell_D$. In this case the equilibrium potential in the mid-plane vanishes, $\psi_{eq,m} = 0$, and the EDL's do not interact at equilibrium. The coefficients of the transport matrix \mathbf{t} , at the exception of $t_{vv} = \tilde{z}^3/12$, are all affine functions of \tilde{z} and write as the sum of a bulk part proportional to \tilde{z} and of a surface part: $t_{ij} = a_{ij}\tilde{z} + b_{ij}$ (see Appendix). More specifically the bulk part of t_{ee} is due to molecular diffusion only, while the bulk part of t_{ve} corresponds to the bulk electro-osmotic flow and depends only on the surface potential ψ_s :

$$a_{ee} = \kappa \quad a_{ve} = \frac{\psi_s}{4} = \frac{1}{2} \operatorname{asinh} \frac{\alpha}{2} \quad (5.1)$$

The surface parts b_{ee} and b_{ve} correspond to transports in the EDL's and their detailed expression as a function of κ and α is given in Appendix.

In these conditions the function $t_{ve}^2/t_{vv}(t_{vv}t_{ee} - t_{ve}^2)$ to integrate in order to get \mathcal{Z}_{EK} is a rational fraction whose denominator is an always positive fourth degree polynomial. The non-dimensional EK damping writes:

$$\mathcal{Z}_{EK} = \frac{144}{a_{ee}} \sum_{i=1}^4 \frac{A_i}{a_i^2} \left[\left(\frac{\tilde{D}}{a_i} - 1 \right) \ln \left(1 - \frac{a_i}{\tilde{D}} \right) + 1 - \frac{a_i}{2\tilde{D}} \right] \quad (5.2)$$

where the function \ln is the complex logarithm, the a_i 's are the four complex roots of $t_{vv}t_{ee} - t_{ve}^2$, and the complex coefficients A_i 's obey the relations:

$$A_i = \frac{(a_{ve}a_i + b_{ve})^2}{\prod_{j \neq i} (a_i - a_j)} \quad \sum_{i=1}^4 A_i = \sum_{i=1}^4 \frac{A_i}{a_i^2} = \sum_{i=1}^4 \frac{A_i}{a_i^3} = 0 \quad \sum A_i a_i = a_{ve}^2$$

We find numerically that the analytical expression (5.2) holds up to $\tilde{D} \sim 4$. At very large

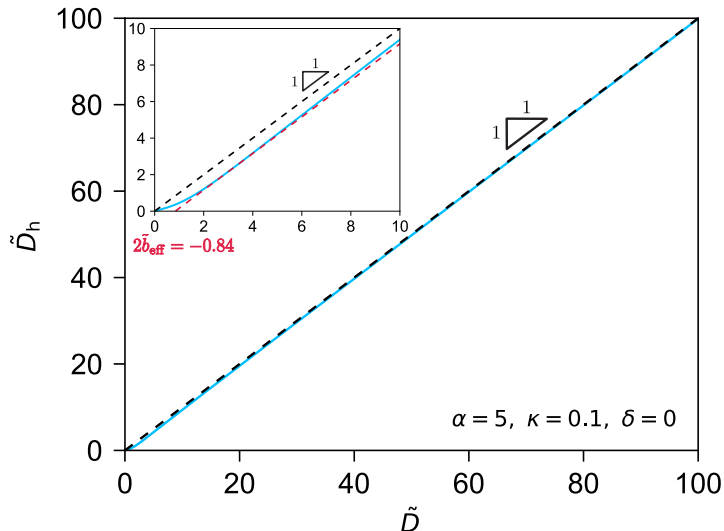


Figure 2: Normalized hydrodynamic distance $\tilde{D}_h = D_h/2\ell_D = \tilde{D}/(1 + \mathcal{Z}_{EK}/\mathcal{Z}_{Reynolds})$ as a function of \tilde{D} , for $\alpha = 5$, $\kappa = 0.1$ and $\delta = 0$. The dashed line is the diagonal $\tilde{D}_h = \tilde{D}$. Inset: expansion in the distance range $\tilde{D} \leq 10$. The red dashed line corresponds to $\tilde{D}_h = \tilde{D} + 2b_{eff}/2\ell_D$ with $b_{eff} = -0.84\ell_D$.

distance the leading term of \mathcal{Z}_{EK} is in $1/\tilde{D}^3$ as first calculated by Bike & Prieve (1990):

$$\mathcal{Z}_{EK} \simeq \frac{12a_{ev}^2}{a_{ee}\tilde{D}^3} = \frac{3\psi_s^2}{4\kappa\tilde{D}^3} \quad \mathcal{Z}_{EK} = i\omega \frac{R^2\ell_D^2}{\ell_B D^3} \frac{3eV_s}{D_s} \quad (5.3)$$

Experimentally it can be of interest to characterize the excess damping due to the electro-kinetic effect by an hydrodynamic distance between the surfaces, defined as $D_h = 6\pi\eta\omega R^2/\Im(Z)$. Indeed when the damping reduces to the Reynolds damping, D_h is the distance separating the no-slip planes. In presence of an excess damping, the hydrodynamic distance reflects the virtual position of the solid surfaces that would produce an equivalent Reynolds damping, in other words it accounts for the excess dissipation by (apparent) stagnant layers at wall of thickness $b_{app} = (D - D_h)/2$. Figure 2 shows a typical plot of the hydrodynamic distance versus the real distance, showing actually $D_h < D$. In a range of distance of some tens of Debye's length, the difference of $D - D_h$ is non-negligible and corresponds to apparent stagnant layers of the order of the Debye length. However these apparent stagnant layers are not constant, their thickness decreases and decays to zero when $\tilde{D} \rightarrow \infty$. This is in agreement with the expansion of \mathcal{Z}_{EK} at large \tilde{D} which has no \tilde{D}^{-2} term ($(\tilde{D} - 2b_{app})^{-1} \sim \tilde{D}^{-1} + 2b_{app}\tilde{D}^{-2}$ at $\tilde{D} \rightarrow \infty$). Thus the electro-kinetic effect, although it induces an increased dissipative mechanism whose origin lies in the surface charge and the EDL's, cannot be described by a well-defined and non-ambiguous hydrodynamic distance based on apparent stagnant fluid layers at the solid walls.

5.2. Small and intermediate distances.

At $\tilde{D} < 1$ the EDL's overlap. One observes on figure 3 a quasi-saturation of \mathcal{Z}_{EK} . In this case a simplified model for the thin electrolyte film is the so-called Donnan's model,

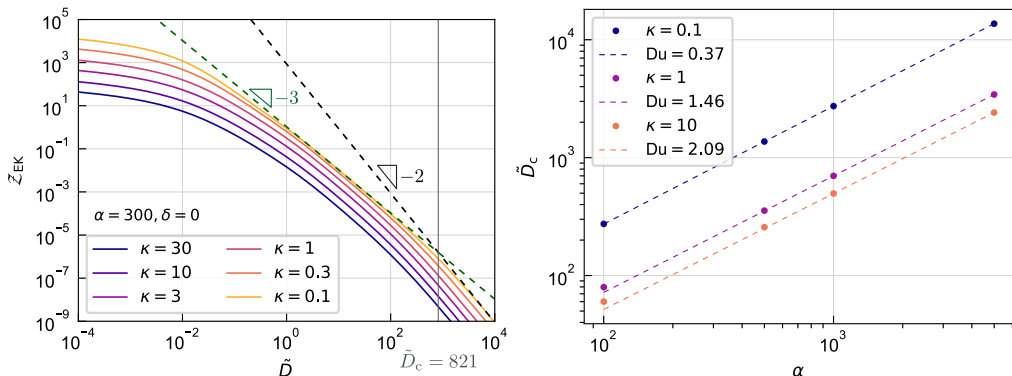


Figure 3: Left: Adimensional electrokinetic damping \mathcal{Z}_{EK} as a function of the normalized distance $\tilde{D} = D/2\ell_D$ for the parameter $\alpha = 300$, $\delta = 0$, and various values of κ . The dashed line of slope -3 plots the scaling law (5.3), the dashed line of slope -2 plots the scaling law (5.5). Right: crossing distance \tilde{D}_c between the power laws in \tilde{D}^{-2} and in \tilde{D}^{-3} followed by \mathcal{Z}_{EK} , as a function of α . The dashed lines correspond to the values of the Dushin number given by equation 5.6.

explicited in Appendix E. The electro-kinetic factor becomes to the leading order:

$$\frac{t_{ve}^2}{t_{vv}(t_{vv}t_e - t_{ve}^2)} \simeq \frac{\alpha}{\tilde{z}^2\kappa(1-\delta)} \quad \mathcal{Z}_{EK} \simeq -\frac{\alpha \ln \tilde{D}}{\kappa(1-\delta)} \quad (5.4)$$

At $\tilde{D} > 1$, figure 3 shows that an intermediate behaviour develops at high enough surface charge, not following the \tilde{D}^{-3} asymptotic power law (5.3), but rather a \tilde{D}^{-2} power law. In this distance range the EDL's do not overlap ; but this intermediate behaviour is due to the fact that the electrical conduction of the electrolyte film is dominated by the counter-ions of the EDL's rather than the bulk solution: $t_{ee} \approx b_{ee}$. This occurs when $\tilde{z} < |b_{ee}/a_{ee}| = \alpha[\gamma(1 + 1/2\kappa) - \delta]$. In this range of distance the electrokinetic damping writes:

$$\mathcal{Z}_{EK} \simeq \int_{\tilde{D}}^{\infty} d\tilde{z} \int_{\tilde{z}}^{\infty} \frac{144a_{ve}^2}{b_{ee}^2\tilde{z}'^6} d\tilde{z}' = \frac{24a_{ve}^2}{b_{ee}\tilde{D}^2} \quad (5.5)$$

This scaling law is fully supported by the data as shown in figure 3.

The dominance of the EDL's conduction in a film of thickness h is generally characterized by the Dushin number $Du = \sigma/2nh$. In our case the Dushin number at thickness z is $Du = \alpha/\tilde{z}$. The crossing distance between the intermediate regime described by the law (5.5) and the large distance power law (5.3) is indeed expected to occur at $\tilde{D}_c = b_{ee}/2a_{ee}$, that is a Dushin number $Du_c = 2\alpha a_{ee}/b_{ee}$, expressing as (see Appendix D):

$$\tilde{D}_c = \frac{\alpha}{2} \left[\gamma \left(1 + \frac{1}{2\kappa} \right) - \delta \right] = \frac{\alpha}{Du_c} \quad Du_c = 2 \left[\gamma + \frac{\gamma}{2\kappa} - \delta \right]^{-1} \quad (5.6)$$

The comparison of this law to the cross-over distance determined from the numerical data in figure 3 right, supports fully the interpretation of the intermediate range of \mathcal{Z}_{EK} in terms of Dushin number and dominance of the electrical conduction of the EDL's.

5.3. Comparison to the Reynolds damping

We use the relative amplitude factor $\tilde{f}_{EK} = (\tilde{D}/6)\mathcal{Z}_{EK}$ defined in equation 4.13 to compare the electro-kinetic damping to the Reynolds damping.

Figure 4 top-left shows the influence of the diffusion parameter κ on \tilde{f}_{EK} . Without

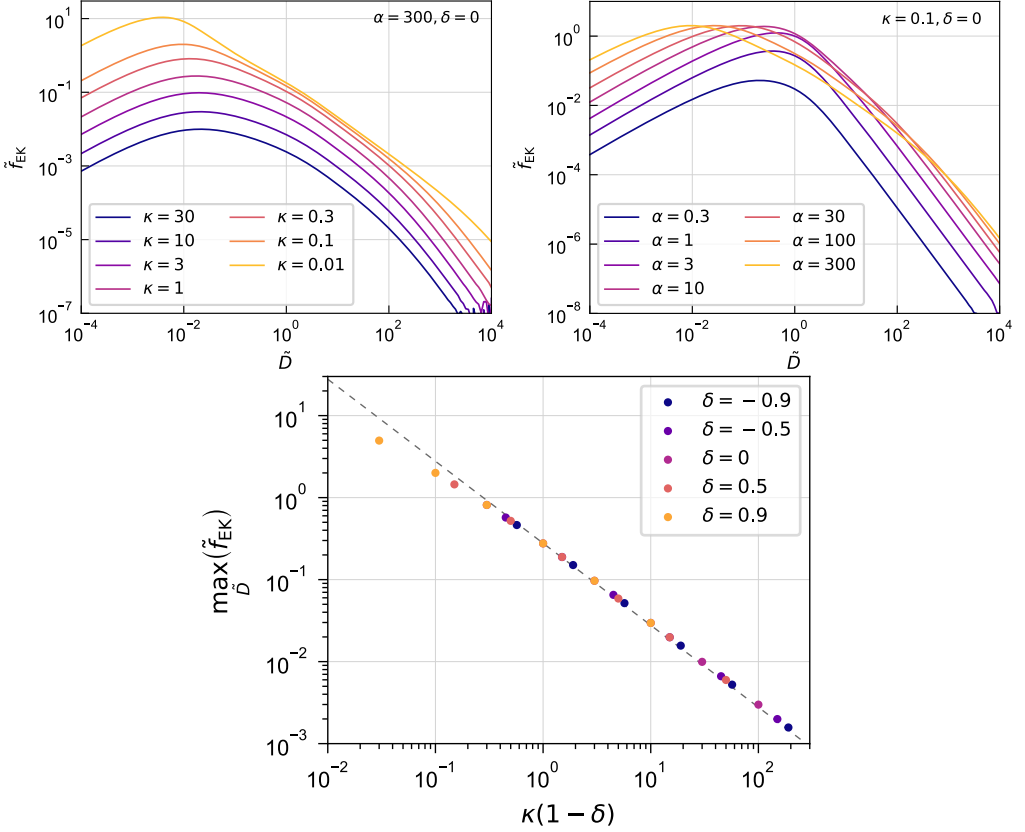


Figure 4: Top left: relative electro-kinetic damping $\tilde{f}_{EK} = \mathcal{Z}_{EK}\tilde{D}/6$ as a function of the normalized distance $\tilde{D} = D/2\ell_D$ for $\alpha = 300$, $\delta = 0$, and various values of κ . Top right: \tilde{f}_{EK} as a function of \tilde{D} for $\kappa = 0.1$, $\delta = 0$, and various values of α . Bottom: maximum value of the relative electrokinetic damping \tilde{f}_{EK} , for $\alpha > 50$, as a function of the normalized diffusion coefficient of the counter-ions $\kappa(1 - \delta)$. Values of the diffusion contrast δ are reported in the legend. Values of κ can be read on the x-axis at $\delta = 0$, and are (0.3,1,3,10,30,100). The maximum value of \tilde{f}_{EK} does not depend on α .

surprise \tilde{f}_{EK} decreases when κ increases, as this corresponds to an increase of the electrolyte conductivity, and therefore a decrease of the electric field required to restore the global electro-neutrality. In the regions of very strong overlap ($\tilde{f}_{EK} \sim D \ln D$) and of non-overlap with small Dushin ($\tilde{f}_{EK} \sim 1/D^2$) \tilde{f}_{EK} decreases essentially in $1/\kappa$. In the intermediate distance range however, \tilde{f}_{EK} saturates to a diffusion-independent limit at low κ . This effect is due to the main contribution of the electro-osmotic flow to the electrolyte conductivity in this range of film thickness at low diffusivity and large surface charge.

Figure 4 top-left shows the influence of the electrical parameter α on \tilde{f}_{EK} . At small values of α the relative amplitude of the electro-kinetic damping increases with the surface charge, as expected intuitively. However above $\alpha \geq 10$ (for the particular value of $\kappa = 0.1$), the maximum value reached by \tilde{f}_{EK} becomes totally independent of α . The only effect of increasing α is that the maximum of \tilde{f}_{EK} is reached for lower and lower distances. This effect is in fact associated to a non-monotonic variation of \tilde{f}_{EK} with α at a given distance \tilde{D} . For α values large enough so that the intermediate distance range of high

Dushin number (with $\tilde{f}_{EK} \sim D^{-1}$) develops, \tilde{f}_{EK} is a decreasing function of α . The amplitude of \tilde{f}_{EK} in this intermediate distance range is indeed determined by the ratio α_{ve}^2/b_{ee} (see equation 5.5), which is in fact the square of the amplitude of the bulk electro-osmotic flow, divided by the contribution of this flow to the electrical conductivity. Clearly the bulk electro-osmotic flow grows as $\psi_{s,nominal} \sim \ln \alpha$, whereas its contribution to the conductivity grows as $\alpha\gamma \sim \alpha$ at high surface charge (see Appendix D for the expression of b_{ee}). Therefore, the increase of conductivity dominates in the intermediate regime, and induces the inversion of growth of \tilde{f}_{EK} with α .

Finally the overall maximum value of the relative electro-kinetic damping is plotted in figure 4 bottom for values of $\alpha \geq 50$. A remarkable variation is found as the inverse of the normalized diffusion coefficient of the counter ions, $\kappa(1 - \delta)$. This behaviour reflects the fact that the properties of overlapping EDL's are determined by the ones of the counter-ions. Electro-kinetic dampings may reach 100% of the Reynolds damping for $\kappa(1 - \delta) \leq 0.3$, which means counter-ions of hydrodynamic radius slightly less than 0.4 nm (in water at 300K). This property of the maximum relative electro-kinetic damping could provide a method for measuring quite accurately the diffusion coefficient of single ionic species.

6. Properties of the diffusio-kinetic impedance

The diffusio-kinetic impedance is calculated by solving numerically the linear differential equation (4.11) and integrating equation (4.10). These operations are performed all-at-once using Python ODE solving routines, details of implementation and codes are reported in the Supplementary Materials.

6.1. Diffusio-kinetic stiffness

The diffusio-osmotic stiffness $\Re Z_{DK}$ takes its origin in ions accumulation, as described by the r.h.s of equation (c).

High frequency upper limit at $\omega \geq \omega_c \kappa$.

At high frequency the ions follow adiabatically the motion of the sphere: the perturbation in ion concentration is fully in phase with the displacement, and both the modification of the disjunction pressure as well as the diffusio-osmotic flow are in phase with the displacement. The additional pressure Π_{DK} needed to counter-balance the diffusio-osmotic flow is thus also in phase with the displacement. In this high frequency limit the diffusio-kinetic stiffness is frequency-independant and takes the analytic form:

$$\Re m_s^{hf} = \frac{g + g'(z - \tilde{D}) - a(\tilde{z})}{b(\tilde{z})} \quad (6.1a)$$

$$\Re Z_{DK}^{hf} = \int_{\tilde{D}}^{\infty} d\tilde{z} \left((g - a) \Re m_s^{hf} + \int_{\tilde{z}}^{\infty} g' \Re m_s^{hf} d\tilde{z}' \right) \quad (6.1b)$$

which is calculated by a simple integration (see Sup. Mat).

Figure 5 left shows a typical plot of the variation of $\Re(Z_{DK})$ as a function of \tilde{D} for $(\alpha, \kappa) = (10, 1)$ and various values of $\beta = \omega/\omega_c$. We observe that for all the distance range, the high frequency behaviour is an upper limit for the diffusio-kinetic stiffness: $\Re Z_{DK} \leq \Re Z_{DK}^{hf}$. This property holds for all parameters α and κ , therefore the highest possible values of the stiffness are always obtained when the convergence to the high-frequency limit is reached.

In practice we observe that the convergence is essentially reached when $\omega/\omega_c \kappa \geq 1$. This appears on figure 5 left for the particular value $(\alpha, \kappa) = (10, 1)$, and tests with

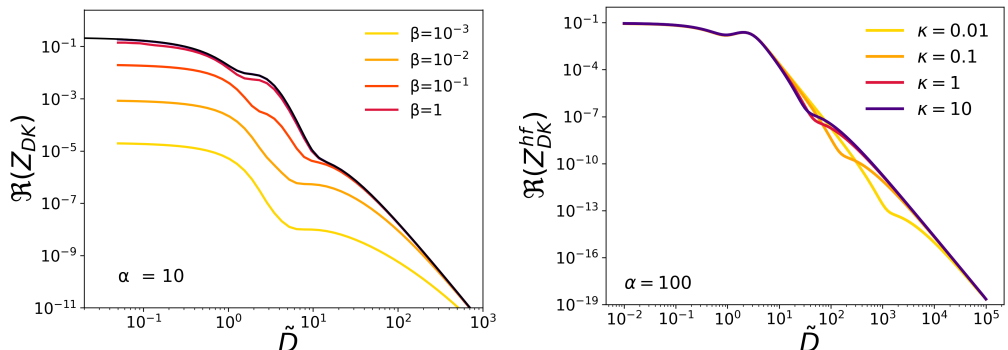


Figure 5: Left: real part of the diffuso-kinetic impedance $\Re(Z_{DK})$ as a function of the adimensional gap $\tilde{D} = D/2\ell_D$, for $\alpha = 10$, $\kappa = 1$ and various values of $\beta = \omega/\omega_c$. The black line correspond to the high frequency limit eq. (6.1b). Right: high frequency stiffness $\Re(Z_{DK}^{hf})$ as a function of \tilde{D} for $\alpha = 100$ and various values of κ .

various values of (α, κ) fully support this property. The time $(\omega_c \kappa)^{-1} = R\ell_D/2D_s$ indeed represents the molecular diffusion time over the lateral extension $\sqrt{2R\ell_D}$ of the overlapping EDL's when $\tilde{D} = 0$. This time is the shortest system's time found on the route toward restoring the equilibrium, therefore when it is larger than the oscillation period, the high frequency limit is reached.

Finally the convergence toward the high frequency limit is not uniform over the distance range, and occurs for lower frequencies at large distances. More specifically the convergence at distance \tilde{D} is essentially obtained for $\omega \simeq D_s/R\ell_D\tilde{D}$, which is the inverse of the diffusion time over the lateral extension of the hydrodynamic contact $\sqrt{2RD}$.

Long-range decay and comparison with the DLVO stiffness

At large distance when EDL's do not overlap, $dN_s \simeq 2z(n - n_o)$, thus $a(\tilde{z}) \simeq 0$ and $b(\tilde{z}) \simeq 2\tilde{z}$. The transport coefficients t_{ij} are affine functions of \tilde{z} except for $t_{vv} \simeq \tilde{z}^3/12$, and $g(\tilde{z})$ resume to the leading order to g_2/\tilde{z}^2 , $g_2 = 12a_{vs}$ if $\delta = 0$. The high-frequency stiffness has the asymptotic form:

$$\Re Z_{DK}^{hf} \sim \frac{42a_{vs}^2}{5\tilde{D}^4} \quad a_{vs} = -\frac{1}{2} \ln(1 - \gamma^2) \quad (6.2)$$

In this large distance regime, the long range decay of the stiffness in $1/D^4$ is fully due to the transport of the excess ions concentration in the EDL's by the Poiseuille flow and the resulting diffuso-osmotic flow thereby induced. The long range decay depends only on the surface charge α and does not involve any diffusion process.

At short distance the stiffness saturates (see figure 5 right) to a value which is also independent of diffusion. As a whole the influence of diffusion in the high-frequency stiffness appears only in the intermediate range $1 < \tilde{D} < \alpha$, that is when the EDL's do not overlap but the Dushin number is larger than 1. In this intermediate range the excess ions in the EDL's play a more important role in the transport properties than the bulk, resulting in an interplay between convective and diffusive transport. Note that the stiffness decays quite fast and only the short distance behaviour up to $\tilde{D} = 10$ might fall in an experimental range.

It is of interest to compare the diffuso-kinetic stiffness to the DLVO stiffness, which for $\tilde{D} > 1$ decreases exponentially with \tilde{D} . As the dimensional prefactor is in $Rn_o k/BT$ for both quantities, this comparison can be made on the non-dimensional expressions

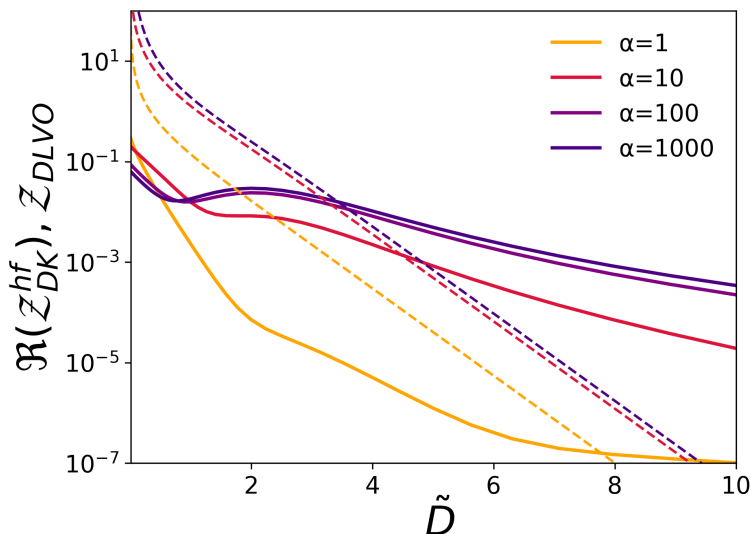


Figure 6: Plain lines: non-dimensional high-frequency diffusio-kinetic stiffness $\Re \mathcal{Z}_{DK}^{hf}$ for various values of α . The diffusion contrast δ is set to 0. Dashed lines: non-dimensional DLVO stiffness $\mathcal{Z}_{DLVO} = Z_{DLVO}/8\pi R n_o k_B T$ for $\alpha = 1$ (yellow), $\alpha = 10$ (red), and $\alpha = 100$ (indigo). For higher values of α the DLVO stiffness is essentially the same as for $\alpha = 100$.

of the stiffness, and is independent on the sphere radius. One sees on figure (6) that at distance sufficiently large the diffusio-kinetic stiffness always exceeds the DLVO stiffness. Furthermore the inversion of magnitude occurs essentially at a distance where the high-frequency diffusio-kinetic stiffness does not depend on κ . For the $\alpha = 1$ the crossing distance is about $\tilde{D} = 8$, at a very low value of the stiffness, and should not be possible to reach experimentally. However for higher values of α the crossing distance decreases and the stiffness values increases significantly, reaching somewhat typical distance values $\tilde{D} \sim 3.5 - 4$ and stiffness value $\sim 0.05 \times 8\pi R n_o k_B T$ at $\alpha > 20$.

6.2. Diffusio-kinetic damping

Variations with frequency.

The real and imaginary part of m_s being related as (see eq 4.11):

$$\Im m_s = -\frac{\omega_c}{\omega b(\tilde{z})} \frac{d}{d\tilde{z}} \left((\tilde{z} - \tilde{D}) h(\tilde{z}) \frac{d\Re m_s}{d\tilde{z}} \right)$$

the diffusio-kinetic damping converges at high frequency towards a function of \tilde{D} strictly proportional to ω_c/ω . This property is evidenced in figure 7 left, showing that the quantity $(\omega/\omega_c)\Im \mathcal{Z}_{DK}$ reaches a frequency-independant limit at high frequencies. The dependency in $1/\omega$ of $\Im \mathcal{Z}_{DK}$ stems from the fact that at high frequency the transport of ions is "frozen" and reversible as it follows the surfaces motion, thus the damping ultimately vanishes. The convergence of $(\omega/\omega_c)\Im \mathcal{Z}_{DK}$ towards its high-frequency limit follows fully the scheme of the diffusio-kinetic stiffness: the limit is essentially obtained for $\omega/\kappa\omega_c \geq 1$, and the departure from the limit occurs first at small distances $D < D_s/R\omega$, as was observed on the stiffness (see figure 7 left).

In the lower frequency range, the damping reverses its frequency variation and becomes

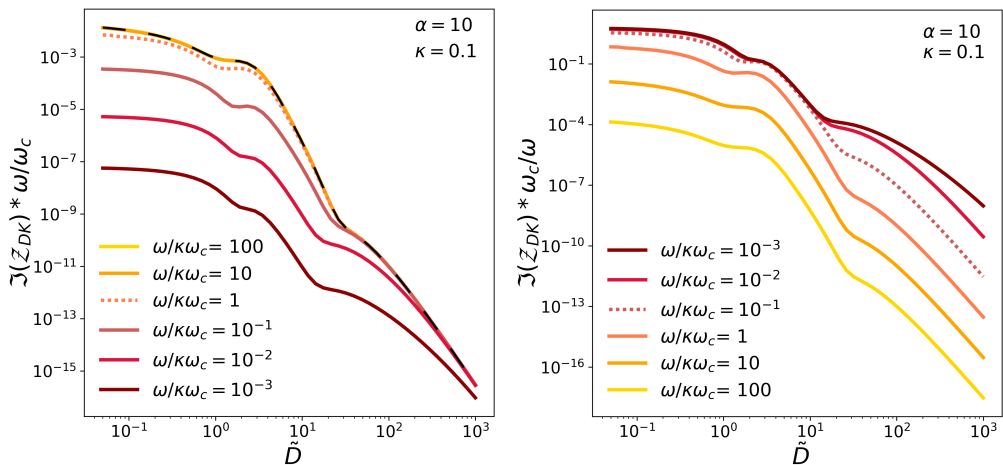


Figure 7: Left: imaginary part of the diffusio-kinetic impedance multiplied by the frequency ratio $\Im(\mathcal{Z}_{DK}) * \omega/\omega_c$ as a function of the adimensional gap $\tilde{D} = D/2\ell_D$, for $\alpha = 10$, $\kappa = 0.1$ and various values of $\omega/\kappa\omega_c$. For values $\omega/\kappa\omega_c \geq 1$ all the data are very close to, or collapse on the black dashed line. Right: imaginary part of the diffusio-kinetic impedance divided by the frequency ratio $\Im(\mathcal{Z}_{DK}) * \omega_c/\omega$ as a function of \tilde{D} for the same values of α , κ and $\omega/\kappa\omega_c$ as on the left graph. For values $\omega/\kappa\omega_c \leq 10^{-1}$ all the data in the range $\tilde{D} \leq 10$ collapse on the same plot.

proportional to ω . It thus recovers the usual damping feature of being proportional to the forced velocity. As shown on figure 7 right, the quantity $(\omega_c/\omega)\Im\mathcal{Z}_{DK}$ which governs the relative damping factor \tilde{f}_{DK} (see equation 4.12) reaches a low frequency limit $[(\omega_c/\omega)\Im\mathcal{Z}_{DK}]^{lf}$ when $\omega \rightarrow 0$. This low frequency limit appears to be an upper limit over all the distance range, and for all parameters (α, κ). Therefore the highest possible values of the diffusion-kinetic damping factor \tilde{f}_{DK} are always obtained when the convergence of $(\omega_c/\omega)\Im\mathcal{Z}_{DK}$ to its low-frequency limit is reached.

Figure 7 right shows the typical features of the convergence. When ω is decreased, the small distance range converges first, before the high distance range. For most parameters the full convergence is obtained for $\omega/\omega_c \leq 0.1\kappa$ in the distance range $\tilde{D} \leq 10$. Thus the diffusio-kinetic damping factor \tilde{f}_{DK} reaches its maximum value \tilde{f}_{DK}^{lf} at $\tilde{D} \leq 10$ for $\omega/\omega_c \leq 0.1\kappa$.

Comparison to the Reynolds damping

In the following we compare the diffusio-kinetic damping to the Reynolds damping by plotting the relative factor $\tilde{f}_{DK} = (\omega_c/\omega)\Im\mathcal{Z}_{DK}\tilde{D}/6$ at its maximum value, that is at frequencies $\omega = 0.1\omega_c\kappa$ or lower.

Figure 8 top plots the diffusio-kinetic factor \tilde{f}_{DK} obtained for various surface charges at a typical $\kappa = 0.1$. The factor shows two peak values at distances $\tilde{D} \sim 0.4$ and $\tilde{D} \sim 3$, the second being more important in amplitude. The amplitude of the second peak increases with the surface charge, and saturates for large values $\alpha \geq 100$, where the maximum diffusio-kinetic damping reaches about 30% of the Reynolds damping. For comparison with the electro-kinetic damping, the factor \tilde{f}_{EK} is plotted in dashed-line in figure 8. The diffusio-kinetic damping is in general significantly lower than the electro-kinetic one. However it is of interest to note that due to the charge inversion effect in the

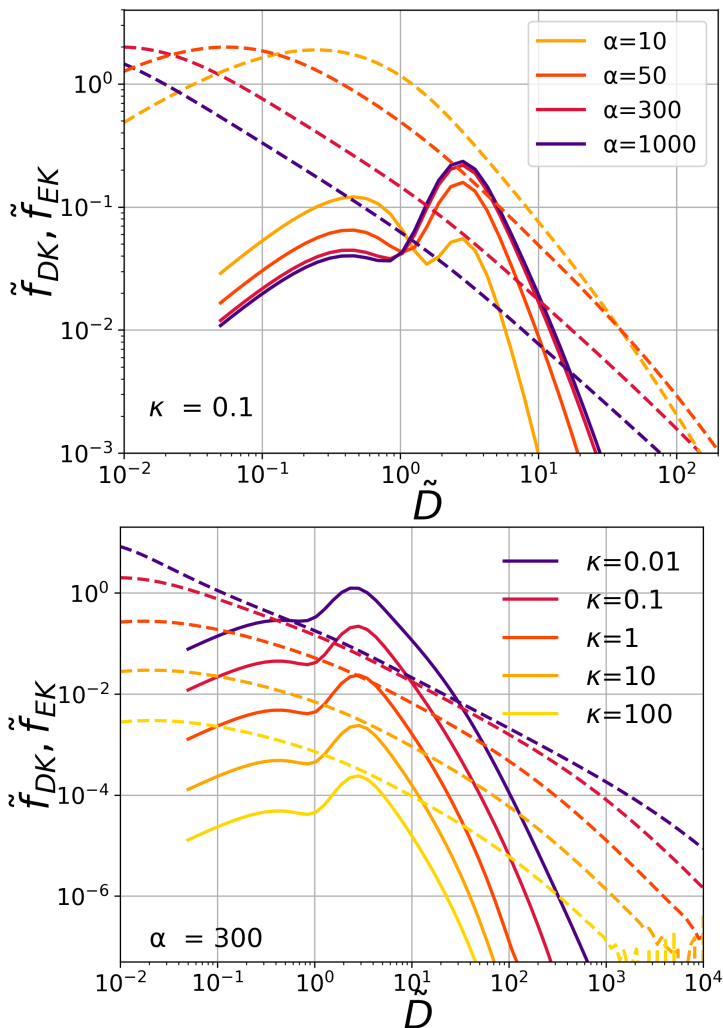


Figure 8: Left: imaginary part of the diffusio-kinetic impedance multiplied by the frequency ratio $\Im(\mathcal{Z}_{DK}) * \omega/\omega_c$ as a function of the adimensional gap $\tilde{D} = D/2\ell_D$, for $\alpha = 10$, $\kappa = 0.1$ and various values of $\omega/\kappa\omega_c$. For values $\omega/\kappa\omega_c \geq 10$ all the data collapse on the black dashed line. Right: imaginary part of the diffusio-kinetic impedance $\Im(\mathcal{Z}_{DK})$ as a function of \tilde{D} for the same values of α , κ and $\omega/\kappa\omega_c$ as on the left graph.

electro-kinetic damping, the diffusio-kinetic factor \tilde{f}_{DK} may become comparable and even dominant over \tilde{f}_{EK} , for $\alpha \geq 50$ and in the distance range $1 \leq \tilde{D} \leq 10$.

Figure 8 down plots the diffusio-kinetic factor \tilde{f}_{DK} at the rather high value of $\alpha = 300$ for various values of κ . We observe that \tilde{f}_{DK} increases as κ decreases, a trend already observed in the electro-kinetic damping and due to the restauring character of molecular diffusion. However the variation of \tilde{f}_{DK} is very regular in $1/\kappa$, and does not show an intermediate distance range of large Dushin number where the effect of diffusion saturates at low κ , as it occurs for the electro-kinetic damping. Therefore, the diffusio-kinetic factor exceeds the electro-kinetic factor at $\kappa \geq 1$ in the range $2\ell_D < D < 20\ell_D$, and may reach 100% of the Reynolds damping at $\kappa = 0.01$.

In summary the main features of the diffusio-kinetic impedance are:

- a long-range stiffness decaying in $1/D^4$, frequency-independant for $\omega \geq D_s/R\ell_D$, and susceptible to overcome the DLVO stiffness at $\tilde{D} \gtrsim 4$
- a damping in most of the cases negligible, but that can overcome the electro-kinetic damping and even reach the level of the Reynolds damping if three conditions are met: a low frequency $\omega \leq 0.1D_s/R\ell_D$, a high parameter $\alpha = 2\ell_D/\ell_G \leq 50$ (i.e. nominal surface potential $\psi_s \sim 200$ mV), and ions of large hydrodynamic radius $r_H \leq \ell_B$.

7. Conclusion

In this paper, we develop a semi-analytical model for hydrodynamic forces in electric double layers within the linear response regime, considering the drainage of a thin liquid film confined by dielectric solids. We assume the film to be at equilibrium along its thickness, which holds for an ionic aqueous solution at a concentration of 10 μM or greater ($\lambda_D = 100$ nm or lower) when the working frequency is small compared to 100 kHz.

Unlike Mugele and collab., who do not take into account the transport of ions by convection in their model – which can be legitimate when using microscopic probes – we consider here all coupled transports of volume, charge and solute (Zhao *et al.* 2020). Hence, we find that, when the lateral diffusion of ions cannot follow the excitation frequency, convection takes over and the hydrodynamic force exhibits a conservative component arising from the emerging diffusio-osmotic flow. Yet, this conservative diffusio-osmotic force, which had never been calculated before, may be significant in experiments compared to the DLVO force when ionic diffusion is low, as in ionic liquids.

Furthermore, we provide an analytical calculation of the additional electro-hydrodynamic viscous force with respect to a dielectric liquid, of which Mugele and collab. has provided a semi-analytical calculation from an integral expression. We also find that the additional viscous force stemming from diffusio-osmotic effects is in most cases negligible with respect to the previous one.

We find that the additional electro-hydrodynamic viscous force does not vary monotonically with the surface charge and vanishes for highly charged surfaces. We demonstrate that this highly counterintuitive effect arises from the divergence of the conductivity of electrolyte liquid films at small thicknesses due to the contribution of counterions. More intuitively, this additional force increases as ion diffusion decreases, with ions playing an asymmetric role depending on the sign of their charge: the diffusion of counter-ions – relative to the sign of the surface charge – predominates that of co-ions.

Finally, our theory provides a means to measure the surface charge governing diffusio-electrokinetic transport phenomena – assumed to be constant and unique, though these constraints can be relaxed – which can then be directly compared to the DLVO surface charge without any adjustable parameters. We therefore believe that a direct confrontation of this model with experiments could lead to a better understanding of what the ill-defined concept of surface charge encompasses.

Acknowledgements. We thank Lydéric Bocquet for many helpful discussions. We thank Abdelhamid Maali for pointing to us the work of Bike & Prieve (1990).

Funding. This work has been funded by the french Agence Nationale pour la Recherche under the grant number ANR-19-CE30-0012-01.

Appendix A. Consequences of the Derjaguin approximation

A.1. Electric field in the dielectric solids

The potential ψ in the dielectric spheres satisfies the harmonic equation $\Delta\psi = 0$ with the boundary condition $\psi = \psi_s$ at the surface of the spheres. Far from the polar axis, ψ_s is uniform, determined by the surface potential of the solid immersed in the electrolyte solution, and ψ is also uniform. Close to the Oy axis the two spheres may come into electrostatic interaction, and $\psi_s(r)$ is no longer constant. But in the Derjaguin approximation this occurs only in a region where the sphere surfaces are almost parallel, that is perpendicular to Oy . Therefore the harmonic equation is solved in the half-space $y \geq z/2$, neglecting the variation of z with r . The solution is:

$$\psi(r, y) = \int_0^\infty e^{-s(y-z/2)} \tilde{\psi}_s(s) J_0(sr) s \, ds \quad \tilde{\psi}_s(s) = \int_0^\infty J_0(sr) \psi_s(r) r \, dr$$

where J_0 is the Bessel function of the first kind and 0th order. The normal and tangential fields in the sphere at the level of the surface are:

$$\frac{\partial\psi}{\partial y}\Big|_{z/2^+} = - \int_0^\infty \tilde{\psi}_s(s) J_0(sr) s^2 \, ds \quad \frac{\partial\psi}{\partial r}\Big|_{z/2} = - \int_0^\infty \tilde{\psi}_s(s) J_1(sr) s^2 \, ds$$

Therefore the normal electric field inside the sphere is of same magnitude as the tangential electric field. The latter is negligible in the electrolyte at the level of the surface, due to the Derjaguin approximation. Thus in equation (2.5d) the normal field inside the sphere can be neglected.

A.2. General expression of the force

We start from equation (2.11), and note that due to the flow incompressibility and the no-slip boundary condition, at $y = z/2$ we have $\partial v_y / \partial y = -(1/r)(\partial(rv_r)/\partial r) = 0$.

Taking the y component of the Stokes equation (2.3d), replacing in it $(n^+ - n^-)$ according to the Poisson equation (2.9), and neglecting the radial component $\Delta_r v_y$, we obtain the relation:

$$0 = -\frac{\partial P}{\partial y} + \eta \frac{\partial^2 v_y}{\partial y^2} + \frac{k_B T}{4\pi\ell_B} \frac{\partial^2 \psi}{\partial y^2} \frac{\partial \psi}{\partial y} \quad (\text{A1})$$

(A1) is integrated along y with the boundary conditions (2.4) and the incompressibility relation to find:

$$\left[-P + \frac{k_B T}{8\pi\ell_B} \left(\frac{\partial\psi}{\partial y} \right)^2 \right] \left(r, \left(\frac{z}{2} \right)^- \right) = - \left[P + \frac{\eta}{r} \frac{\partial r v_r}{\partial r} \right] (r, 0) \quad (\text{A2})$$

so that the force (2.11) resumes to:

$$F = \int_0^\infty 2\pi r P(r, 0) dr + 2\pi\eta \lim_{r \rightarrow \infty} [r v_r(r, 0)] \quad (\text{A3})$$

The magnitude of the second term in the above expression can be estimated from

$$\eta |r v_r| \propto \eta |r \frac{dv_r}{dr}| = \eta |r^2 \frac{dv_y}{dy}| \propto \eta | \frac{r^2 \dot{D}}{z} | \rightarrow \eta R \dot{D} \quad \text{when } r \rightarrow \infty$$

This term is negligible with respect to the first one whose magnitude is of order $\eta \frac{R^2 \dot{D}}{D}$.

A.3. Invariance of Π across the film thickness

By injecting equation (3.7) in the Stokes equation (2.3d) we get

$$\eta \nabla^2 \vec{v} = \vec{\nabla}(P - k_B T n_s) + e n_e \vec{\nabla} W + n_s \vec{\nabla} \mu_s \simeq \eta \frac{\partial^2 v_y}{\partial y^2}$$

as $\Delta_r \ll \partial^2/\partial y^2$. The fields W and μ_s and their gradient are uniform in the section, therefore projecting the above equation on y reads $\partial \Pi / \partial y = \eta \partial^2 v_y / \partial y^2$. By integrating this equation over y and derivating the result against r , taking into account $\partial v_y / \partial y = -(1/r)(\partial v_r / \partial r)$, we see that the magnitude of the variation of $\partial \Pi / \partial r$ in the y direction is of the order of $\eta \Delta_r v_r$. Therefore at the level of the current approximations the field $\partial \Pi / \partial r$ is uniform across the liquid film in eq. (3.8d).

Appendix B. Elements of the transport matrix

From equations (3.8b,3.8c) one defines the diffusive part of the concentration and charge fluxes as:

$$J_{s,\text{diff}} = -\frac{D_s}{k_B T} \frac{d\mu_s}{dr} \int_0^{z(t)/2} (n_s + n_e \delta) dy - \frac{e D_s}{k_B T} \frac{dW}{dr} \int_0^{z(t)/2} (n_e + n_s \delta) dy$$

$$J_{s,\text{diff}} = -\frac{D_s}{k_B T} \frac{d\mu_s}{dr} [N_s + n_o z + N_e \delta] - \frac{e D_s}{k_B T} \frac{dW}{dr} (N_e + (N_s + n_o z) \delta)$$

$$J_{e,\text{diff}} = -\frac{D_s}{k_B T} \frac{d\mu_s}{dr} (N_e + (N_s + n_o z) \delta) - \frac{e D_s}{k_B T} \frac{dW}{dr} ((N_s + n_o z) \delta)$$

One then introduces $v'_r = (\eta/2n_o k_B T) v_r$ and integrate (3.8d) over y using the symmetry boundary condition (2.4) $\partial v_r(y)/\partial y(y=0) = 0$:

$$\eta \frac{\partial v_r(r, y, t)}{\partial y} = \Gamma_v \frac{d\Pi}{dr} + \Gamma_e(r, y, t) \frac{dW}{dr} + \Gamma_s(r, y, t) \frac{d\mu_s}{dr}$$

$$\Gamma_v = \int_0^y dy = y \quad \Gamma_s(r, y, t) = \int_0^y (n_s - 2c) dy \quad \Gamma_e = \int_0^y e n_e dy$$

The volume flux can be expressed as:

$$J_v = \int_0^{z(t)/2} v_r(y) dy = - \int_0^{z(t)/2} y \frac{\partial v_r(y)}{\partial y} dy$$

$$J_v = -\frac{1}{\eta} \left[\frac{d\Pi}{dr} \int_0^{z(t)/2} \Gamma_v^2 dy + \frac{d\mu_s}{dr} \int_0^{z(t)/2} \Gamma_v \Gamma_s(y) dy + \frac{dW}{dr} \int_0^{z(t)/2} \Gamma_v \Gamma_e(y) dy \right]$$

The convective charge flux writes:

$$I = e J_e = \int_0^{z(t)/2} e n_e v_r(y) dy = - \int_0^{z(t)/2} \Gamma_e \frac{dv_r}{dy} dy$$

and the convective ion flux:

$$J_{s,\text{conv}} = 2c J_v + \int_0^{z(t)/2} (n_s - 2c) v_r(y) dy = 2c J_v - \int_0^{z(t)/2} \Gamma_s \frac{dv_r}{dy} dy$$

Altogether the fluxes ($J_v, J_s - cJ_v, I$) are related to the gradients of the potentials Π, μ_s and W by a symmetric transport matrix \mathbf{T} according to:

$$\begin{pmatrix} J_v \\ J_s - cJ_v \\ I \end{pmatrix} = -\mathbf{T} \frac{d}{dr} \begin{pmatrix} \Pi \\ \mu_s \\ W \end{pmatrix} \quad T_{ij} = \int_0^{z(t)/2} \frac{\Gamma_i \Gamma_j}{\eta} dy + \frac{D_s}{k_B T} L_{ij}$$

$$L_{vi} = 0 \quad L_{ss} = \frac{L_{ee}}{e^2} = N_s + n_o z + N_e \delta \quad L_{es} = L_{se} = e(N_e + (N_s + n_o z)\delta)$$

Introducing the local time-dependent Debye's length $\lambda_D = \ell_D e^{-\mu_s/2k_B T}$, and the non-dimensional lengths $\tilde{y} = y/2\lambda_D$, the functions $\Gamma_{s,e}$ express as

$$\Gamma_{s,e} = 4c\lambda_D \tilde{\Gamma}_{s,e} \quad \tilde{\Gamma}_s = \int_0^{\tilde{y}} (\cosh \chi - 1) d\tilde{y}' \quad \tilde{\Gamma}_e = - \int_0^{\tilde{y}} \sinh \chi d\tilde{y}'$$

where χ is the function ψ_{eq} calculated with the boundaries located at $\pm z(t)/2$ and with the local Debye's length λ_D . From (Abramowitz & Stegun (1964)) the $\tilde{\Gamma}_{se}$ express as

$$\Gamma_s(\tilde{y}) = \frac{1}{2\sqrt{k}} \left(2u(1-k) - 2E(u, k^2) + \text{sn}(u, k^2)(k^2 \text{cd}(u, k^2) + \frac{1}{\text{cd}(u, k^2)}) \right) \quad (\text{B 1a})$$

$$\Gamma_e(\tilde{y}) = -\frac{1-k^2}{2\sqrt{k}} \frac{\text{sn}(u, k^2)}{\text{cn}(u, k^2) \text{dn}(u, k^2)} \quad u = \frac{y}{2\lambda_D \sqrt{k}} \quad k = e^{-\chi_m} \quad (\text{B 1b})$$

$$\frac{\alpha \sqrt{k}}{1-k^2} e^{-\mu_s/2k_B T} = \frac{\text{sn}(\tilde{z}(t)/2\sqrt{k}, k^2)}{\text{cn}(\tilde{z}(t)/2\sqrt{k}, k^2) \text{dn}(\tilde{z}(t)/2\sqrt{k}, k^2)} \quad (\text{B 1c})$$

where $E(u, k^2) = E(\phi | k^2)$ is the incomplete elliptic integral of the second kind of parameter k^2 associated to the elliptic integral of the first kind $F(\phi | k^2) = u$, the functions sn, cn, dn are Jacobi elliptic functions, and B 1c is the boundary condition at wall.

Appendix C. Expression of dN_s in the linear response

The ion excess N_s is

$$N_s = 2c \int_0^{z(t)/2} (\cosh \chi - 1) dy + (2c - 2n_o) \frac{z(t)}{2}$$

$$\frac{N_s}{4n_o \ell_D} = e^{\mu_s/2k_B T} \tilde{\Gamma}_s \left(\frac{\tilde{z}(t)}{4\lambda_D \sqrt{k}} \right) + \frac{\tilde{z}(t)}{2} (e^{\mu_s/k_B T} - 1) \quad (\text{C1})$$

The variation of N_s with $z(t)$ and μ_s around equilibrium ($\mu_s = 0$) has to take into account the variation of k with these quantities. The latter is obtained by differentiating the boundary condition B 1c. Introducing the equilibrium potential at the wall $\psi_{eq,s}$ defined by the boundary condition (B 1c) at equilibrium:

$$\alpha = \frac{2\ell_D}{\ell_G} \quad \cosh \psi_{eq,s} = \cosh \psi_{eq,m} + \frac{\alpha^2}{2}$$

one obtains

$$\frac{dk}{k} = -\frac{\frac{h_0}{\ell_D} + \frac{\mu_s}{k_B T} (\tilde{z} + \alpha/2 \sinh \psi_s)}{A} \quad A = \tilde{z} - \frac{2E(\tilde{z}/2\sqrt{k})}{\sqrt{k} \sinh \psi_m} - \frac{2}{\alpha} \left(1 - \frac{\sinh \psi_m}{\sinh \psi_s} \right) \quad (\text{C2})$$

Then by differentiating (C 1) and using the reduced field $m_s = \frac{\mu_s \ell_D}{k_B T h_0}$ one obtains:

$$\frac{dN_s}{2n_o h_0} = \frac{a(\tilde{z})}{2} + m_s \frac{b(\tilde{z})}{2} \quad (\text{C 3a})$$

$$a(\tilde{z}) = \cosh \psi_m - 1 + \frac{\sinh \psi_m}{A(\tilde{z})} \left(\tilde{z} + \frac{\alpha}{\sinh \psi_s} \right) \quad (\text{C 3b})$$

$$b(\tilde{z}) = \frac{\tilde{z}}{2} \left(\frac{3}{k} + k \right) - \frac{2}{\sqrt{k}} E \left(\frac{\tilde{z}}{2\sqrt{k}} \right) - \frac{\alpha^3}{2 \sinh \psi_s} + \frac{2}{\alpha} (\sinh \psi_s - \sinh \psi_m) + \frac{\sinh \psi_m}{A(\tilde{z})} \left(\tilde{z} + \frac{\alpha}{\sinh \psi_s} \right)^2 \quad (\text{C 3c})$$

Here the potentials are equilibrium potentials and $\tilde{z} = z/2\ell_D$.

Finally when the EDL's do not overlap, $\sinh \psi_m = 0$, $\cosh \psi_m = 1 = k = E(z/4\ell_D\sqrt{k})$, $\sinh \psi_s = \alpha\sqrt{1 + \alpha^2/4}$. Introducing $\gamma = \tanh \psi_s/4$ one finds that dN_s reduces to:

$$\frac{dN_s}{2n_o h_0} = m_s \left(\tilde{z} + \frac{1}{\sqrt{1 + \ell_D^2/\ell_G^2}} - 1 \right) = m_s \left(\tilde{z} - \frac{2\gamma^2}{1 + \gamma^2} \right) \quad (\text{C 4})$$

$$a(\tilde{z}) = 0 \quad b(\tilde{z}) = 2\left(\tilde{z} - \frac{2\gamma^2}{1 + \gamma^2}\right) \quad (\text{C 5})$$

Appendix D. Transport coefficients in the non-overlapping regime

Non-overlapping EDL's are treated as single surfaces in solutions, with the Gouy-Chapmann theory giving the reduced potential ψ_{eq} solution of the Poisson-Boltzmann equation with vanishing potential in the mid-plane $\psi_{eq,m} = 0$. In the following we write $\psi_{eq} = \psi$ to lighten the expressions and note $\tilde{y} = y/2\ell_D$:

$$\frac{d\psi}{d\tilde{y}} = 4 \sinh \frac{\psi}{2} \quad \sinh \frac{\psi_s}{2} = \frac{\ell_D}{\ell_G} = \frac{\alpha}{2} = \frac{2\gamma}{1 - \gamma^2} \quad (\text{D 1})$$

$$t = \tanh \frac{\psi(\tilde{y})}{4} = \gamma \exp(2\tilde{y} - \tilde{z}) \quad \gamma = \tanh \frac{\psi_s}{4} = \frac{2}{\alpha} \left(\sqrt{1 + \frac{\alpha^2}{4}} - 1 \right) \quad (\text{D 2})$$

$$\tilde{\Gamma}_s(\tilde{y}) = \int_0^{\tilde{y}} (\cosh \psi - 1) d\tilde{y}' = \cosh \frac{\psi}{2} - 1 \quad \tilde{\Gamma}_e(\tilde{y}) = -\sinh \frac{\psi}{2} = -\frac{d\psi}{4d\tilde{y}} \quad (\text{D 3})$$

With these expressions it is possible to perform analytically the integrals $\int_0^{\tilde{z}/2} \tilde{y} \tilde{\Gamma}_{s,e} d\tilde{y}$ and $\int_0^{\tilde{z}/2} \tilde{\Gamma}_{s,e} \tilde{\Gamma}_{s,e} d\tilde{y}$ and we find $t_{ij} = a_{ij}\tilde{z} + b_{ij}$ (except for $t_{vv} = \tilde{z}/12$) as:

$$a_{ss} = a_{ee} = \kappa \quad a_{se} = \kappa\delta \quad a_{vs} = -\frac{1}{2} \ln(1 - \gamma^2) \quad (\text{D 4})$$

$$a_{ve} = -\frac{1}{2} \ln \frac{1 + \gamma}{1 - \gamma} = -\frac{\psi_s}{4} \quad (\text{D 5a})$$

$$b_{ve} = \frac{1}{2} (\text{Li}_2(\gamma) - \text{Li}_2(-\gamma)) \quad b_{vs} = -\frac{\text{Li}_2(\gamma^2)}{4} \quad (\text{D 5b})$$

$$b_{ee} = \frac{2\gamma^2}{1 - \gamma^2} \left(1 + 2\kappa \left(1 - \frac{\delta}{\gamma} \right) \right) \quad b_{se} = \ln \frac{1 + \gamma}{1 - \gamma} - \frac{2\gamma}{1 - \gamma^2} [1 + 2\kappa(1 - \delta\gamma)] \quad (\text{D 5c})$$

$$b_{ss} = 2 \ln(1 - \gamma^2) + \frac{2\gamma^2}{1 - \gamma^2} \left(1 + 2\kappa \left(1 - \frac{\delta}{\gamma} \right) \right) \quad (\text{D 5d})$$

where $\text{Li}_2(x) = -\int_0^x \frac{\ln(1-u)}{u} du$ and $\text{Li}_2(1-x) = f(x) = -\int_1^x \frac{\ln u}{u-1} du$ is the dilogarithm function f defined by Abramowitz & Stegun (1964) page 1005 paragraph 27.7.

Appendix E. Donnan's model

A simplified model for the thin electrolyte film is the so-called Donnan's model Donnan (1924) whereby the ions concentration and the electrical potential are considered uniform in the thickness, satisfying globally the Boltzmann law $n_{eq}^{\pm} = n_o e^{\pm\psi_D}$ and the electroneutrality condition. The Donnan potential $\psi_{D,eq}(z)$ in the electrolyte film of thickness z is given by

$$\sinh \psi_{D,eq}(z) = Du = \frac{\sigma}{en_o z} = \frac{\alpha}{\tilde{z}} \quad (\text{E1})$$

Within this model the quantities $\tilde{T}_{s,e}$ resume to $\tilde{T}_s(\tilde{y}) = \tilde{y}(\cosh \psi_{D,eq}(z) - 1)$, $\tilde{T}_e(\tilde{y}) = -\tilde{y} \sinh \psi_{D,eq}(z)$, and the transport coefficient t_{ij} write as:

$$t_{ve} = -\sinh \psi_D \frac{\tilde{z}^3}{12} = -\frac{\alpha \tilde{z}^2}{12} \quad t_{vs} = (\cosh \psi_D - 1) \frac{\tilde{z}^3}{12} \quad (\text{E2})$$

$$t_{ee} = \sinh^2 \psi_D \frac{\tilde{z}^3}{12} + \kappa \tilde{z} (\cosh \psi_D - \delta \sinh \psi_D) = \frac{\alpha^2 \tilde{z}}{12} + \kappa (\tilde{z} \cosh \psi_D - \delta \alpha) \quad (\text{E3})$$

$$t_{ss} = (\cosh \psi_D - 1)^2 \frac{\tilde{z}^3}{12} + \kappa (\tilde{z} \cosh \psi_D - \delta \alpha) \quad (\text{E4})$$

$$t_{se} = -\cosh \psi_D \frac{\alpha \tilde{z}^2}{12} + \kappa (\tilde{z} \delta \cosh \psi_D - \alpha) \quad (\text{E5})$$

The Donnan's model is considered to reflect adequately the transport properties when the Dushin number is larger than 1, that is when \tilde{z} is sufficiently small so that $\alpha/\tilde{z} \geq 1$. The transport coefficients can be further simplified as:

$$t_{vs} \simeq -t_{ve} = \frac{\alpha z^2}{12} \quad t_{ee} \simeq t_{ss} \simeq -t_{es} = \frac{\alpha^2 z}{12} + \kappa \alpha (1 - \delta) \quad (\text{E6})$$

REFERENCES

- ABRAMOWITZ, M. & STEGUN, I.A. 1964 *Handbook of Mathematical Functions with Formulas, Graphs, and Mathematical Tables*. U.S. Government Printing Office.
- ANDERSON, J.L. 1989 Colloid transport by interfacial forces. *Annu. Rev. Fluid Mech.* **21**, 61–99.
- BEHRENS, S.H. & GRIER, D.G. 2001 Giant osmotic energy conversion measured in a single transmembrane boron nitride nanotube. *J Chem Phys* **115**, 6716.
- BIKE, S. G. & PRIEVE, D. C. 1990 Electrohydrodynamic lubrication with thin double layers. *Journal of Colloid and Interface Science* **136** (1), 95–112.
- BOCQUET, L. 2020 Nanofluidics coming of age. *Nat. Mater.* **19** (3), 254–256.
- BOCQUET, L. & BARRAT, J.-L. 2007 Flow boundary conditions from nano- to micro-scales. *Soft Matter* **3**, 685–693.
- BOCQUET, L. & CHARLAIX, E. 2010 Nanofluidics, from bulk to interfaces. *Chemical Society Reviews* **39** (3), 1073–1095.
- BONTHUIS, D. J. & NETZ, R. R. 2012 Unraveling the combined effects of dielectric and viscosity profiles on surface capacitance, electro-osmotic mobility, and electric surface conductivity. *Langmuir* **28** (46), 16049–16059.
- BOURG, I. C., LEE, S. S., FENTER, P. & TOURNASSAT, C. 2017 Stern layer structure and energetics at mica–water interfaces. *J. Phys. Chem. C* **121** (17), 9402–9412.

- COTTIN-BIZONNE, C., CROSS, B., STEINBERGER, A. & CHARLAIX, E. 2005 Boundary slip on smooth hydrophobic surfaces: Intrinsic effects and possible artifacts. *Phys. Rev. Lett.* **94** (5), 056102.
- DONNAN, F.G. 1924 The theory of membrane equilibria. *Chem. Rev.* **1**, 73–90.
- GARCIA, L., BARRAUD, C., PICARD, C., GIRAUD, J., CHARLAIX, E. & CROSS, B. 2016 Micro-nano-rheometer for the mechanics of soft matter at interfaces. *Review of Scientific Instruments* **87** (11), 113906.
- GONELLA, G., BACKUS, E. H. G., NAGATA, Y., BONTHUIS, D. J., LOCHE, P., SCHLAICH, A., NETZ, R. R., KÜHNLE, A., MCCRUM, I. T., KOPER, M. T. M., WOLF, M., WINTER, B., MELJER, G., CAMPEN, R. K. & BONN, M. 2021 Water at charged interfaces. *Nat Rev Chem* **5** (7), 466–485.
- GROSS, R. J. & OSTERLE, J. F. 1968 Membrane transport characteristics of ultrafine capillaries. *The Journal of Chemical Physics* **49** (1), 228–234.
- HARTKAMP, R., BIANCE, A.-L., FU, L., DUFRÛCHE, J.-F., BONHOMME, O. & JOLY, L. 2018 Measuring surface charge: Why experimental characterization and molecular modeling should be coupled. *Current Opinion in Colloid & Interface Science* **37**, 101–114.
- HORN, R. G., SMITH, D. T. & HALLER, W. 1989 Surface forces and viscosity of water measured between silica sheets. *Chemical Physics Letters* **162**, 404–408.
- ISRAELACHVILI, J. N. 2011 *Intermolecular and Surface Forces*. Academic Press.
- ISRAELACHVILI, J. N. & ADAMS, G. E. 1978 Measurement of forces between two mica surfaces in aqueous electrolyte solutions in the range 0–100 nm. *Journal of the Chemical Society, Faraday Transactions 1: Physical Chemistry in Condensed Phases* **74**, 975–1001.
- LIU, F., KLAASSEN, A., ZHAO, C., MUGELE, F. & VAN DEN ENDE, D. 2018a Electroviscous dissipation in aqueous electrolyte films with overlapping electric double layers. *J. Phys. Chem. B* **122**, 933–946.
- LIU, Y., KAWAGUCHI, T., PIERCE, M. S., KOMANICKY, V. & YOU, H. 2018b Layering and ordering in electrochemical double layers. *J. Phys. Chem. Lett.* **9** (6), 1265–1271.
- LIZÉE, M., COQUINOT, B., MARIETTE, G., SIRIA, A. & BOCQUET, L. 2024 Anomalous friction of supercooled glycerol on mica. *Nat Commun* **15** (1), 6129.
- LYKLEMA, J. 1994 On the slip process in electrokinetics. *Colloids and Surfaces A: Physicochemical and Engineering Aspects* **92** (1-2), 41–49.
- MAALI, A., COHEN-BOUHACINA, T. & KELLAY, H. 2008 Measurement of the slip length of water flow on graphite surface. *Applied Physics Letters* **92** (5), 053101.
- PRIEVE, D. C., ANDERSON, J. L., EBEL, J. P. & LOWELL, M. E. 1984 Motion of a particle generated by chemical gradients. part 2. electrolytes. *Journal of Fluid Mechanics* **148**, 247–269.
- RODRÍGUEZ MATUS, M., ZHANG, Z., BENRAHLA, Z., MAJEE, A., MAALI, A. & WÜRGER, A. 2022 Electroviscous drag on squeezing motion in sphere-plane geometry. *Phys. Rev. E* **105** (6), 064606.
- SIRIA, A., BOCQUET, M.-L. & BOCQUET, L. 2017 New avenues for the large-scale harvesting of blue energy. *Nat Rev Chem* **2017** **1** (11), 1–10.
- SIRIA, A., PONCHARAL, P., BIANCE, A.-L., FULCRAND, R., BLASE, X., PURCELL, S. T. & BOCQUET, L. 2013 Giant osmotic energy conversion measured in a single transmembrane boron nitride nanotube. *Nature* **494** (7438), 455–458.
- SMOLUCHOWSKI, M. 1904 Contribution à la théorie de l'endosmose électrique et de quelques phénomènes corrélatifs. *J. Phys. Theor. Appl.* **3**, 912.
- TABOR, D. & WINTERON, R. H. S. 1969 The direct measurement of normal and retarded van der Waals forces. *Proceedings of the Royal Society of London. A. Mathematical and Physical Sciences* **312**, 435–450.
- WANG, J., LI, H., TAVAKOL, M., SERVA, A., NENER, B., PARISH, G., SALANNE, M., WARR, G. G., VOÏTCHOVSKY, K. & ATKIN, R. 2024 Ions adsorbed at amorphous solid/solution interfaces form Wigner crystal-like structures. *ACS Nano* **18** (1), 1181–1194.
- ZHAO, C., ZHANG, W., VAN DEN ENDE, D. & MUGELE, F. 2020 Electroviscous effects on the squeezing flow of thin electrolyte solution films. *J. Fluid Mech.* **888**, A29.